

Anomalous η/η' decays: the triangle and box anomalies

M. Benayoun¹, P. David¹, L. DelBuono¹, Ph. Leruste¹, H.B. O'Connell²

¹ LPNHE Paris VI/VII, 75252 Paris, France

² Fermilab, PO Box, 500 MS 109, Batavia, IL 60510, USA

Received: 29 June 2003 / Revised version: 17 September 2003 /

Published online: 4 November 2003 – © Springer-Verlag / Società Italiana di Fisica 2003

Abstract. We examine the decay modes $\eta/\eta' \rightarrow \pi^+\pi^-\gamma$ within the context of the hidden local symmetry (HLS) model. Using numerical information derived in previous fits to the $VP\gamma$ and Ve^+e^- decay modes in isolation and the ρ lineshape determined in a previous fit to the pion form factor, we show that all aspects of these decays can be predicted with fair accuracy. Freeing some parameters does not improve the picture. This is interpreted as strong evidence in favor of the box anomaly in the η/η' decays, which occurs at precisely the level expected. We also construct the set of equations defining the amplitudes for $\eta/\eta' \rightarrow \pi^+\pi^-\gamma$ and $\eta/\eta' \rightarrow \gamma\gamma$ at the chiral limit, as predicted from the anomalous HLS Lagrangian appropriately broken. This provides a set of four equations depending on only one parameter, instead of three for the traditional set. This is also shown to match the (two-angle, two-decay-constant) η - η' mixing scheme recently proposed and is also fairly well fulfilled by the data. The information returned from the fits also matches expectations from previously published fits to the $VP\gamma$ decay modes in isolation.

1 Introduction

Interactions and decays of light mesons fit well within the framework of chiral perturbation theory (ChPT) [1]. Strictly speaking, the ChPT framework applies to the octet members of the pseudoscalar sector (π, K, η_8) which behave as Goldstone bosons whose masses vanish at the chiral limit. Relying on the large N_c limit of QCD, an extended ChPT framework (EChPT) has been defined [2, 3] including the singlet η_0 state which keeps a non-zero mass at the chiral limit, but this vanishes in the large N_c limit. On the other hand, the decays $\pi^0/\eta/\eta' \rightarrow \gamma\gamma$, are understood as proceeding from the so-called triangle anomaly. These are accounted for by means of the Wess–Zumino–Witten (WZW) Lagrangian [4, 5] which is also normally incorporated into the ChPT Lagrangian [2, 3].

Other anomalous processes describing the $(\pi^0\pi^+\pi^-\gamma)$ vertex and the decay mode ($\eta \rightarrow \pi^+\pi^-\gamma$) have been identified long ago within the context of current algebra [6]; they are presently referred to as box anomalies. Triangle and box anomalies are now derived from the WZW Lagrangian. The box anomaly part of the WZW Lagrangian predicts exactly the values of the amplitudes for the couplings $(\pi^0\pi^+\pi^-\gamma)$, $(\eta\pi^+\pi^-\gamma)$ and $(\eta'\pi^+\pi^-\gamma)$ at the chiral limit; however, the momentum dependence of the corresponding amplitudes is not predicted and should be modeled. When dealing with experimental data, this momentum dependence is naturally accounted for by vector meson contributions and, then, the question becomes whether these alone account for the box anomalies or whether an additional contact term (possibly simulating high mass

resonances) is needed; if this contact term (CT) is needed, it should have a definite value in order to stay consistent with the rigorous predictions of the WZW Lagrangian.

Therefore, from an experimental point of view, the question of the relevance of the box anomaly phenomenon turns out to check the need for a well-defined contact term besides the usual resonant contributions. This question is still awaiting a definite and unambiguous signature.

In its simplest form, the problem of the relevance of the box anomaly phenomenon is addressed in the coupling $(\pi^0\pi^+\pi^-\gamma)$. The relevance of a possible contact term beside vector meson exchanges has been examined. A value for this coupling has been extracted from experimental data [7] and found to be close to expectations¹ (only 2σ apart).

A cleaner environment could be provided by the decay modes $\eta/\eta' \rightarrow \pi^+\pi^-\gamma$ which are also accounted for in the WZW Lagrangian. Several pieces of information are available: the partial widths [9] are known with an accuracy of the order 10% cross-checked by several means, the η spectrum as a function of the photon momentum has been measured long ago [10, 11] and provides useful information. Finally, measurements of the η' spectrum as a function of the dipion invariant mass have been performed twelve times, with various levels of precision, and the corresponding data have been published as papers from several Collaborations [12–18] or are available as Ph.D. theses [19–22]. The latest measurements have been performed recently by CERN Collaborations [23, 24].

¹ See, also, the discussion in [8]

This already represents a large amount of information covering all aspects of these decays. This should allow a reasonably well founded analysis to be made in a search for the box anomaly in the η/η' system.

As stated above, predictions on box anomalies are given at the chiral point, and η/η' spectra clearly extend in regions where accounting for the ρ exchange cannot be avoided in order to match experimental information. The magnitude of the $\eta/\eta' \rightarrow \pi^+\pi^-\gamma$ partial widths should also be influenced by the ρ exchange. Stated otherwise, including the momentum (invariant mass) dependence within their spectra is essential and should be done in a consistent way in order to reliably extract information on the box anomaly from the data.

Indeed, in these decays, two contributions are a priori competing: a contact term and a (dominant) resonant one – the ρ exchange – with contributions of (sometimes) very different magnitudes. In order to reliably detect the former, the latter has to be known with enough accuracy and, possibly, should be fixed. The sharing in the anomalous amplitudes at the chiral limit between the contact term and the resonant term might also have to be understood unambiguously.

Therefore, a global framework is needed where the vector meson degrees of freedom are explicitly accounted for together with pseudoscalar mesons and the contact terms. Several such frameworks implementing vector dominance (VMD) in effective Lagrangians have been defined: resonance chiral perturbation theory [1, 25], massive Yang–Mills fields [26–28], and the hidden local symmetry (HLS) model [29, 30]. It was soon shown [31] that all these approaches were physically equivalent. For convenience, we work within the HLS model context.

A second issue concerns the difference between the π^0 box anomaly and the η/η' ones. The former is practically insensitive to symmetry breaking effects (isospin symmetry breaking is a small effect), the latter however sharply depends on how SU(3) symmetry and nonet symmetry breakings really take place. Therefore a reliable breaking scheme of the η/η' sector should also be defined and checked in the triangle and box anomaly sectors. It should also be validated in all processes where it has to apply, like $V \rightarrow P\gamma$ and $P \rightarrow V\gamma$ decays. One has already noted some confusion [32] in the meaning of the decay constants entering the amplitudes for the η and η' decays to two photons.

If one limits oneself to collecting some VMD term for the ρ contribution (even if motivated) and simply adds it with a phase space term to be fit, one can be led to ambiguities [33, 34] when solving the Chanowitz equations [35] which represent the traditional way of describing the η/η' mixing (see also [36]). Along the same line, if the breaking scheme generally used [33, 35–38] happens to be inappropriate in order to describe the η/η' system, extracting the box anomaly constant values from the data becomes hazardous.

A scheme for implementing SU(3) symmetry breaking in the full HLS Lagrangian has been already defined [39, 40]. This scheme, referred to as BKY, has been proved [32] to meet all (E)ChPT requirements and allows a successful

account to be given of a very large set of experimental data [41, 42]. A brief global account of the full breaking scheme we advocate is summarized in Appendix A to [43]. The non-anomalous sector has been used in pion form factor studies providing also consistent results [43, 44].

Therefore, in this paper, we intend to extend the realm of the broken HLS model by studying the decays $\eta/\eta' \rightarrow \pi^+\pi^-\gamma$. The behavior of the model can then be examined in a context where the box anomaly phenomenon is expected to be present. One can hope to extract unambiguously the information about the relevance of this phenomenon from the experimental data.

This paper is organized as follows: in Sect. 2 we recall the traditional expressions of the decay amplitudes at the chiral limit for $\eta/\eta' \rightarrow \gamma\gamma$ and $\eta/\eta' \rightarrow \pi^+\pi^-\gamma$. In Sect. 3, we outline the derivation of the full anomalous sector of the HLS model, mostly referring to the basic paper [30]. In Sect. 4 we recall briefly how the BKY breaking of the SU(3) symmetry and the breaking of the nonet symmetry has been performed and tested. In Sect. 5, we recall the result of applying this to $\eta/\eta' \rightarrow \gamma\gamma$ as it provides an unconventional set of expressions for the amplitudes at the chiral limit.

In Sect. 6, we develop the structure predicted for the $\eta/\eta' \rightarrow \pi^+\pi^-\gamma$ decay modes by the broken HLS model. We first show that the BKY breaking scheme provides also unconventional expressions for the box anomaly amplitudes at the chiral limit. We also show that all information related with these decay modes (parameters and ρ meson lineshape) have already been derived numerically and functionally in other sectors of the low energy phenomenology. It thus follows that all properties of the $\eta/\eta' \rightarrow \pi^+\pi^-\gamma$ decay modes can be predicted without any numerical or functional freedom. In Sect. 7, we examine the predictions of this model for the $\eta/\eta' \rightarrow \pi^+\pi^-\gamma$ partial widths and for their dipion invariant-mass spectra.

After reviewing briefly the status of the available experimental data on this subject in Sect. 8, we devote Sect. 9 to comparing the predicted lineshapes with the published experimental spectra. Section 10 is devoted to performing a global fit of the shape and to information for the $\eta/\eta' \rightarrow \pi^+\pi^-\gamma$ modes in order to check precisely the relevance of the numerical parameters which were all fixed from an analysis of other independent data sets. In Sect. 11, we propose, for comparison, fits of the anomalous amplitudes at the chiral limit, under various conditions and show that the one (instead of three as usually) parameter dependence of these gets a strong support from the data.

Finally, Sect. 12 is devoted to a summary of the results obtained and to our conclusions.

2 Radiative decays of neutral pseudoscalar mesons

Some interactions (or decay modes) of neutral pseudoscalar mesons ($P = \pi^0, \eta, \eta'$) are described by matrix elements having the wrong parity and are called anomalous. Anomalous interactions were treated by Wess and

Zumino [4] and then expounded upon by Witten [5]; they are given by the anomalous action, which we shall refer to as Γ_{WZW} . For the purpose of this paper, two pieces² from Γ_{WZW} are relevant:

$$\begin{aligned}\mathcal{L}_{\gamma\gamma P} &= -\frac{N_c e^2}{4\pi^2 f_\pi} \epsilon^{\mu\nu\rho\sigma} \partial_\mu A_\nu \partial_\rho A_\sigma \text{Tr}[Q^2 P], \\ \mathcal{L}_{\gamma PPP} &= -\frac{ieN_c}{3\pi^2 f_\pi^3} \epsilon^{\mu\nu\rho\sigma} A_\mu \text{Tr}[Q \partial_\nu P \partial_\rho P \partial_\sigma P],\end{aligned}\quad (1)$$

with $e^2 = 4\pi\alpha$, and $f_\pi = 92.42 \text{ MeV}$; Q is the quark charge matrix,³ A is the electromagnetic field and P is the bare pseudoscalar field matrix. From this, amplitude intensities at the chiral point can be derived.

The first piece $\mathcal{L}_{\gamma\gamma P}$ describes the decays $\pi^0/\eta/\eta' \rightarrow \gamma\gamma$. The second piece $\mathcal{L}_{\gamma PPP}$ contains an interaction term $\gamma \rightarrow \pi^+\pi^0\pi^-$ as briefly discussed in the Introduction. This last piece contains also terms which account for the anomalous decay modes $\eta/\eta' \rightarrow \pi^+\pi^-\gamma$.

Without introducing symmetry breaking effects, the Lagrangian pieces in (1) can give reliable predictions for processes involving only pions. In order to deal with interactions involving η or η' mesons, one has to feed these Lagrangians with SU(3) and nonet symmetry breaking mechanisms. Usually these breaking mechanisms are considered to arise from the naive replacement of the pseudoscalar decay constants [8, 35–37, 48]. Using an obvious notation, the amplitudes at the chiral point derived from (1) can be written

$$T(X \rightarrow \gamma\gamma) = B_X(0) \epsilon^{\mu\nu\rho\sigma} \epsilon_\mu \epsilon'_\nu k_\rho k'_\sigma,$$

$$T(X \rightarrow \pi^+\pi^-\gamma) = E_X(0) \epsilon^{\mu\nu\rho\sigma} \epsilon_\mu k_\nu p_\rho^+ p_\sigma^- \quad (2)$$

($X = \eta, \eta'$), where the coefficients are, assuming $N_c = 3$,

$$\begin{aligned}B_\eta(0) &= -\frac{\alpha}{\pi\sqrt{3}} \left[\frac{\cos\theta_P}{f_8} - 2\sqrt{2} \frac{\sin\theta_P}{f_0} \right], \\ B_{\eta'}(0) &= -\frac{\alpha}{\pi\sqrt{3}} \left[\frac{\sin\theta_P}{f_8} + 2\sqrt{2} \frac{\cos\theta_P}{f_0} \right], \\ E_\eta(0) &= -\frac{e}{4\pi^2\sqrt{3}} \frac{1}{f_\pi^2} \left[\frac{\cos\theta_P}{f_8} - \sqrt{2} \frac{\sin\theta_P}{f_0} \right], \\ E_{\eta'}(0) &= -\frac{e}{4\pi^2\sqrt{3}} \frac{1}{f_\pi^2} \left[\frac{\sin\theta_P}{f_8} + \sqrt{2} \frac{\cos\theta_P}{f_0} \right],\end{aligned}\quad (3)$$

using the traditional one-angle mixing scheme. The procedure is thus obvious: one replaces one power of f_π by

² Here and in the following, we denote by V the (massive) vector field matrix, by A the electromagnetic field and by P the pseudoscalar field matrix. The matrix normalization we use for these has been defined in [29, 32, 40]; our normalization for the SU(3) flavor matrices differs from those in [8] by a factor of 2: $T_{\text{Holstein}}^\alpha = T_{\text{Witten}} = 2 T_{\text{HLS}}^\alpha$. Moreover, we use without distinction $VP\gamma$ and AVP to denote the corresponding coupling

³ There is an intimate connection between the charge of quarks and the value of N_c in the anomalous action [45–47]; $Q = \text{Diag}(2/3, -1/3, -1/3)$ if $N_c = 3$

the octet (f_8) or singlet (f_0) decay constant understood by their customary definitions in (extended) ChPT. In the following, we refer to $X \rightarrow \gamma\gamma$ and $X \rightarrow \pi^+\pi^-\gamma$ as triangle and box anomalies.

This implies several assumptions which are traditionally made in an implicit way [8, 37]:

- (1) the decay constant f_8 and f_0 are the (usual) decay constants of ChPT defined from current expectation values: $\langle 0|J_\mu^8|\eta_8(q)\rangle = if_8 q_\mu$ and $\langle 0|J_\mu^0|\eta_0(q)\rangle = if_0 q_\mu$;
- (2) SU(3) and nonet symmetry breaking acts in exactly the same way for the triangle and box anomalies.

These equations have been used in several ways and they underlie decades of phenomenological work on the η/η' mixing. For instance, [8, 36, 37] consider the two-photon decay widths of the η and η' mesons and the ratio $f_8/f_\pi \simeq 1.3$ from ChPT [1] to derive $\theta_P \simeq -20^\circ$ and $f_0/f_\pi \simeq 1.04$; this meets ChPT expectations [2, 3] if one identifies θ_P with the presently named θ_8 . Comparable results [34, 38] are derived by using the four equations above, after extracting the box anomaly constants from the dipion mass spectra in $\eta/\eta' \rightarrow \pi^+\pi^-\gamma$ decays. The third one in (3) has also been used with accepted parameter values ($f_8/f_\pi = 1.25$, $f_0/f_\pi = 1.04$ and $\theta_P = -20.6^\circ$) inside the HLS model to derive a successful description of $\eta \rightarrow \pi^+\pi^-\gamma$ in isolation [49].

The validity of the first two equations of (3) has been recently addressed and the consistency of these with the η/η' breaking scheme derived from EChPT [2, 3] has been found to be doubtful [32, 50, 51].

There is no currently known examination of the last two equations in (3); however, some remarks on the renormalization of the WZW box term [40] tend to indicate that these are also doubtful. Therefore, the phenomenological results derived from using (3) have to be reexamined in a consistent framework.

3 The anomalous sector in the HLS model

The HLS model originally describes the γ - V transitions, all couplings of the kind VPP and possibly APP , if the specific parameter a of the HLS model [29] is not fixed in order to recover the traditional VMD formulation ($a = 2$). In this framework, the main decay mode $\omega \rightarrow \pi^+\pi^0\pi^-$ of the ω meson is, for instance, absent as is clear from the explicit expression of the HLS Lagrangian [40].

As seen above, anomalous interactions involving pseudoscalar mesons and photons are contained in Γ_{WZW} [4, 5]. These terms were included in the hidden local symmetry Lagrangian by Fujiwara et al. [30], along with anomalous vector meson (V) interactions in such a way that the low energy anomalous processes (in the chiral limit where $m_\pi = 0$) $\gamma \rightarrow \pi^+\pi^0\pi^-$ and $\pi^0 \rightarrow \gamma\gamma$ are solely predicted by Γ_{WZW} . The construction of this HLS anomalous Lagrangian, originally performed in [30], is discussed in detail in several excellent reviews [28, 39]. Here, we limit ourselves to a brief outline of its derivation, pointing out the motivation for some important assumptions. The anomalous

action has the form

$$\Gamma = \Gamma_{\text{WZW}} + \Gamma_{\text{FKTUY}} ,$$

$$\Gamma_{\text{FKTUY}} = \sum_{i=1}^4 c_i \int d^4x \mathcal{L}_i , \quad (4)$$

where the c_i are entirely arbitrary constants. The Lagrangians \mathcal{L}_i are given in [30] and each of them contains *APPP* and *AAP* pieces which would contribute to the anomalous decays, but are cancelled by *APV* terms. These Lagrangians contain also *VPPP* and *VVP* pieces [30].

In view of extending the assumption of the dominance of vector mesons (VMD) to the anomalous sector, it was first shown that a set of c_i in (4) can be defined in such a way that $\pi^0 \rightarrow \gamma\gamma$ occurs solely through $\pi^0 \rightarrow \omega\rho^0$ followed by the (non-anomalous) transitions $\omega \rightarrow \gamma$ and $\rho^0 \rightarrow \gamma$. The π^0 width thus derived is identical to the current algebra prediction reproduced by $\mathcal{L}_{\gamma\gamma P}$ defined in the previous section.

It was also shown [30] that complete vector dominance can be achieved, where the direct term *APPP* is converted to *VPPP*, with some other set of c_i . In this framework, the decay $\omega \rightarrow \pi^+\pi^0\pi^-$ occurs through $\omega \rightarrow \pi^0\rho^0$ (the *VVP* term) followed by $\rho^0 \rightarrow \pi^+\pi^-$ and through the contact term (*VPPP*) which gives a direct contribution $\omega \rightarrow \pi^+\pi^0\pi^-$. However, it happens that the *VVP* contribution (which provides alone the correct ω partial width) is numerically reduced in a significant way by the contact term (*VPPP*). In view of this, [30] proposes another set of c_i which provides an anomalous effective Lagrangian containing only a *VVP* term and, besides, the standard WZW term *APPP* in the following combination:

$$\mathcal{L}^{\text{FKTUY}} = -\frac{3g^2}{4\pi^2} \epsilon^{\mu\nu\rho\sigma} \text{Tr}[\partial_\mu V_\nu \partial_\rho V_\sigma P] - \frac{1}{2} \mathcal{L}_{\gamma P P P} , \quad (5)$$

where $\mathcal{L}_{\gamma P P P}$ is defined in (1). One should note that the normalization affecting the WZW part of this Lagrangian is a pure prediction of the HLS model based on a definite extension of the VMD concept to anomalous processes.

Focussing on decays like $\eta/\eta' \rightarrow \pi^+\pi^-\gamma$, one readily sees from this expression that, in order to recover the behavior expected from $\mathcal{L}_{\gamma P P P}$ alone, these two terms should contribute to the box anomaly (i.e. the full amplitude at the chiral limit) in the following ratio:

$$\text{VMD} : \text{CT} = -3 : 1 ,$$

at the chiral limit; “VMD” here denotes the contribution generated by the first term in (5) and “CT” (contact term) those generated from the second term. Thus, the “VMD” contribution, generated by the triangle anomaly generalized to the *VVP* couplings, is predicted to be dominant at the chiral limit.

Within this framework, the main ω decay mode proceeds only from $\omega \rightarrow \rho^0\pi^0$ followed by $\rho^0 \rightarrow \pi^+\pi^-$ and $\phi \rightarrow \pi^+\pi^-\pi^0$ proceeds solely from ω - ϕ mixing. The experimental situation concerning the decay mode $\phi \rightarrow \pi^+\pi^-\pi^0$ is conflicting. Indeed, a recent result from the SND Collaboration [52] claims no significant evidence in favor of

a contact $\phi \rightarrow \pi^+\pi^-\pi^0$ term in their $e^+e^- \rightarrow \pi^+\pi^-\pi^0$ data and provides a new upper bound much more stringent than previous ones [9]; however, using their own data on the same physical process, the KLOE Collaboration [53] claims that a significant contact term is present in their data. Actually, as there is currently no analysis available performed using consistently a full *VVP* and *VPPP* Lagrangian or a Lagrangian like in (5), no founded conclusion can really be drawn.

Processes like $\pi^0/\eta/\eta' \rightarrow \gamma\gamma$ occur solely through $\pi^0/\eta/\eta' \rightarrow VV'$ followed by $V, V' \rightarrow \gamma$. However, transitions like $\gamma \rightarrow \pi^+\pi^0\pi^-$ or decays like $\eta/\eta' \rightarrow \pi^+\pi^-\gamma$ receive contributions from the contact term and from the *VVP* term (essentially through ρ meson exchange).

The *VVP* piece of this effective Lagrangian has been used successfully in several recent studies [32,41,42,55] and proved to predict (after implementing appropriate symmetry breaking mechanisms) up to 26 pieces of physics information with a number of free independent parameters ranging from 6 to 9 (when isospin symmetry breaking is considered [55]).

4 The extended BKY symmetry breaking scheme

The study of SU(3) breaking of the HLS model has been initiated by BKY [39] who proposed a simple and elegant mechanism. However, the procedure was soon understood as breaking also the Hermiticity of the derived Lagrangian, which was clearly an undesired feature. A slight modification [40] of the original BKY procedure was shown to cure this problem and to produce a quite acceptable broken Lagrangian (see (A5) in [40]). The way field renormalization has to be performed turns out to define the renormalized field matrix (denoted P') in terms of the bare field matrix (denoted P) by

$$P = X_A^{-1/2} P' X_A^{-1/2} , \quad (6)$$

where the breaking matrix is $X_A = \text{Diag}(1, 1, z)$, with $z = [f_K/f_\pi]^2$.

As such, the (original) BKY breaking scheme can only address a limited amount of physics processes, as all information related with the η meson can only be treated crudely, and the properties of the η' meson cannot be addressed.

In order to address the question of physical information on the η/η' system appropriately, the singlet sector has first to be introduced in the original HLS Lagrangian. This has been done by using [40] the U(3) symmetric field matrix $P = P_8 + P_0$ instead of only $P = P_8$ when constructing the Lagrangian. This is found to provide the HLS Lagrangian with the canonical kinetic energy of the singlet state (η_0 field) while this does not modify the interaction Lagrangian [40] by adding η_0 -dependent pieces.

The step further is to break the $U_A(1)$ symmetry by introducing determinant terms [56] into the effective La-

grangian which becomes [32]

$$\mathcal{L} = \mathcal{L}_{\text{HLS}} - \frac{1}{2}\mu^2\eta_0^2 + \frac{1}{2}\lambda\partial_\mu\eta_0\partial^\mu\eta_0. \quad (7)$$

By means of this (modified) BKY breaking scheme, the HLS Lagrangian can now address the η/η' system with a complete scheme of symmetry breaking (SU(3) and nonet symmetries). A η_0 mass term is generated and the kinetic energy term of the Lagrangian is modified in a non-canonical way, which implies that a field transformation to renormalized fields has to be performed. This can be done through the two-step renormalization procedure defined in [32] and outlined in the Appendix. This transformation is well approximated [32] by

$$P = X_A^{-1/2}[P'_8 + xP'_0]X_A^{-1/2}; \quad (8)$$

this has been shown to differ [32] from the exact field transformation only by terms of second order in the breaking parameters ($[z-1]$, $[x-1]$).

This transformation⁴ was postulated (or fortunately anticipated) in [41] in order to study the full set of AVP radiative decays, especially the modes involving the η/η' mesons. Using this transformation has provided a fairly good description all physics accessible to this broken Lagrangian [32, 41, 42, 55] with only a small number of parameters, as already noted.

Departures from nonet symmetry were observed [41] by extracting from data $x = 0.90 \pm 0.02$, significantly different from 1. One may raise the question of the correspondence between x in (8) and the basic nonet symmetry breaking parameter λ of the Lagrangian in (7) – which is [32] nothing but the A_1 parameter of [2, 3]. One can write

$$x = \frac{1}{\sqrt{1+h\lambda}}, \quad h = 1 + \mathcal{O}(z-1). \quad (9)$$

Indeed, as shown in the Appendix, x absorbs a small influence of SU(3) symmetry breaking (about 5% of its fitted value).

Comparison of all results of this broken HLS Lagrangian, especially decay constants and mixing angles, with the available (E)ChPT estimates of the same parameters [2, 3, 50] was done and also appeared to be fully satisfactory. It is worth remarking that the HLS phenomenology was yielding an estimate for the (E)ChPT mixing angle θ_0 much smaller in magnitude than the (E)ChPT leading order estimate ($-0.05^\circ \pm 0.99^\circ$ in contrast with $\simeq -4^\circ$), but in fair correspondence with a more recent EChPT next-to-leading order calculation [58] which yields $\theta_0 = [-2.5^\circ, +0.5^\circ]$.

It is also worth remarking that the (full) breaking scheme just outlined anticipated [41] a branching frac-

tion for $\phi \rightarrow \eta'\gamma$ with a value twice smaller than its contemporary measurement [54]. This predicted value coincides with all recent measurements performed with larger statistics [9].

The quasi-vanishing of θ_0 has two interesting consequences. On the one hand, it allows one to relate the traditional wave-function mixing angle with the recently defined θ_8 mixing angle [2, 3] by providing $\theta_8 \simeq 2\theta_P$ (fulfilled at a few percent level); the derivation is given in the Appendix for the exact field transformation.

On the other hand, the condition $\theta_0 = 0$ relates the nonet symmetry breaking parameter x to θ_P :

$$\tan\theta_P = \sqrt{2}\frac{(1-z)}{2+z}x. \quad (10)$$

This relation is fulfilled with a high degree of numerical accuracy [32] and only reflects that the ChPT mixing angle θ_0 is not significantly affected by symmetry breaking effects. This relation will be somewhat refined (see Sect. 11 and the Appendix).

It then follows that from the three originally free breaking parameters associated with the pseudoscalar sector (z , x , θ_P), only one remains unconstrained. It could be either of x or θ_P ; however, it will be shown that x might be preferred.

We do not go on discussing here symmetry breaking in the vector meson sector as it is not in the stream of the present paper; we refer interested readers to [39–42] where this is discussed in detail.

Some remarks are of relevance. The combined nonet symmetry and SU(3) breaking scheme of the HLS Lagrangian presented in this section defines what we name the extended BKY breaking scheme. It restores the relevance of a one angle mixing scheme for the η/η' system. However, this does not give any support to the traditional breaking scheme as expressed by (3). In contrast, it matches fairly well all expectations of the two-angle, two-coupling constant mixing scheme recently derived from EChPT [2, 3, 50, 51] at leading order in the breaking parameters.

This full breaking scheme is also mathematically equivalent to the recently proposed [50, 51] breaking in the quark flavor basis framework; it might be preferred as a definite concept like nonet symmetry breaking, which underlies some Lagrangian pieces (\mathcal{L}_2) of EChPT, can be implemented more clearly, and tracing its effect in phenomenology is easier.

5 Two-photon decay widths of the η and η' mesons

The two-photon decay widths of the η and η' mesons can be derived easily from the HLS Lagrangian (the VVP part of (5)) supplemented by the $V\gamma$ transition amplitudes of the non-anomalous HLS Lagrangian) after renormalizing to physical fields by (8). Applying directly the same (8) to the WZW Lagrangian $\mathcal{L}_{\gamma\gamma P}$ in (1) leads exactly to the

⁴ The motivation behind this postulate was that weighting differently the singlet and octet parts of the P and V field matrices allows one to derive the most general parametrization [57] of the $VP\gamma$ coupling constants consistent with only SU(3) symmetry in the vector and pseudoscalar sectors, while the corresponding U(3) symmetries are both broken

same result⁵ [32]:

$$\begin{aligned}
G_\eta(0) &= -\frac{\alpha}{\pi\sqrt{3}f_\pi} \left[\frac{5z-2}{3z} \cos\theta_P - \sqrt{2} \frac{5z+1}{3z} x \sin\theta_P \right], \\
G_{\eta'}(0) &= -\frac{\alpha}{\pi\sqrt{3}f_\pi} \left[\frac{5z-2}{3z} \sin\theta_P + \sqrt{2} \frac{5z+1}{3z} x \cos\theta_P \right].
\end{aligned} \tag{11}$$

These expressions compare well with the corresponding quantities in (3). However, this correspondence is only formal as defining \bar{f}_8 and \bar{f}_0 by

$$\frac{\bar{f}_\pi}{\bar{f}_8} = \frac{5z-2}{3z}, \quad \frac{\bar{f}_\pi}{\bar{f}_0} = \frac{5z+1}{6z} x, \tag{12}$$

yields $\bar{f}_8 = 0.82f_\pi$ (and $\bar{f}_0 = 1.17f_\pi$), which has little to do with numerical expectations from ChPT (extended or not). It was proved in [32] that these are *not* the standard EChPT decay constants. These can be derived from our broken Lagrangian, yielding information which matches [32] fairly well the EChPT expectations [2, 3].

This proved the basic consistency of the breaking scheme presented in the previous section with EChPT. The formulation given in (11) could look, at leading order, more tractable than present standard expressions; it makes it indeed much clearer that the number of parameters to be determined phenomenologically is limited.

Therefore, the first basic assumption which underlies the understanding of (3) is not fulfilled by the BKY breaking scheme [39, 40], and this is independent of whether nonet symmetry is broken.

Let us remind the reader that (11) give the two-photon radiative decay widths of the η/η' mesons with good accuracy. These can even be predicted by using solely the value of x extracted from the fit to the (independent) set of AVP decay modes of light mesons [32]. Fixing $z = [f_K/f_\pi]^2$ to its experimental value and assuming (10), (11) becomes a constrained system depending on only one parameter and can be solved providing results consistent with using, instead, the AVP decay mode information.

Of course, the mixing angle θ_P entering (11) does not coincide with θ_8 and is derived [32] as $\theta_P = -10.32^\circ \pm 0.20^\circ$ when requiring the constraint (10) to hold exactly; the corresponding value for $\theta_8 \simeq -20^\circ$ compares well to the expectations [1–3]. One should note a recent estimate of $\theta_P = -10^\circ \pm 2^\circ$ provided by lattice QCD computations [59] which strongly supports this phenomenologically extracted value.

Therefore, the picture represented by (11), which does not meet traditional expectations [8, 34, 38, 58], matches quite well all relevant information from ChPT and QCD, and, last but not least, corresponds to a satisfactory description of the whole set of two-body radiative decays of light mesons [32, 41, 42].

⁵ From now on, we assume $N_c = 3$

6 The HLS model for $\eta/\eta' \rightarrow \pi^+\pi^-\gamma$ decay modes

Using the effective Lagrangian in (5), the processes $\eta/\eta' \rightarrow \pi^+\pi^-\gamma$ receive VMD contributions from the VVP term and CT contributions from the $\mathcal{L}_{\gamma P P P}$ piece. The purpose of this section is to examine carefully these decay modes. These will also lead us to question the last two (box) anomaly equations (see (3)).

6.1 Basic Lagrangians

Within the HLS model, the VVP part of $\eta/\eta' \rightarrow \pi^+\pi^-\gamma$ involves, beside the ρ meson, the interplay of the ω and ϕ mesons to their decay mode to $\pi\pi$ only.⁶ However, these (isospin violating) couplings are small enough to be safely neglected. Additionally, the ϕ meson is outside the decay phase space of both η and η' mesons, and the accuracy of the data is far from allowing any ω effect to be significant or simply visible in the η' dipion invariant-mass spectrum.

It can be shown [42], that the $VP\gamma$ couplings following from the anomalous sector of the HLS model can be derived from the corresponding ($VP\gamma$) piece of

$$\begin{aligned}
\mathcal{L} &= C \epsilon^{\mu\nu\rho\sigma} \text{Tr}[\partial_\mu(eQA_\nu + gV_\nu)\partial_\rho(eQA_\sigma + gV_\sigma) \\
&\quad \times X_A^{-1/2}(P'_8 + xP'_0)X_A^{-1/2}] ,
\end{aligned} \tag{13}$$

where g is the universal vector coupling of the HLS model [29]. The value for $C = -3/(4\pi^2 f_\pi)$ is fixed by normalizing the AAP term in (13) to the corresponding WZW Lagrangian in (1).

This equation could essentially be considered as a way to postulate VMD for VVP couplings and it also gives the normalization shown in (5). Focussing on the piece of (13) related with neutral pseudoscalar mesons, one gets

$$\begin{aligned}
\mathcal{L}_{\gamma P^0} &= -\frac{eg}{4\pi^2 f_\pi} \left[\frac{1}{2}\pi^0 + \frac{\sqrt{3}}{2}\eta_8 + x\sqrt{\frac{3}{2}}\eta_0 \right] \epsilon^{\mu\nu\alpha\beta} \partial_\mu A_\nu \partial_\alpha \rho_\beta^0 ,
\end{aligned} \tag{14}$$

with obvious notations. The ρ meson decay relevant for the present study is driven by

$$\mathcal{L}_{\rho\pi\pi} = i\frac{ag}{2}\rho_\mu^0 [\pi^-\partial^\mu\pi^+ - \pi^+\partial^\mu\pi^-] \tag{15}$$

which can be extracted from the non-anomalous (broken or not) HLS Lagrangian. The parameter a is the specific HLS parameter expected such that $a = 2$ in traditional formulations of VMD, but it has always been fitted in the range $a = 2.3 \div 2.5$ from radiative and leptonic decays of light mesons [41, 42] and in pion form factor studies [44, 60]. We recall that the ρ mass in the HLS model is not free

⁶ Indeed, the non-anomalous HLS Lagrangian, broken or not [40], contains no couplings like $\eta\pi V$ or $\eta'\pi V$. Therefore, terms like $\eta/\eta' \rightarrow \pi V$ followed by $V \rightarrow \pi\gamma$ do not contribute to the decays under examination

and is given by the (extended) KSFR relation $m_\rho^2 = ag^2 f_\pi^2$ which does not coincide with traditional mass values [9] ($\simeq 830$ MeV versus $\simeq 775$ MeV); these happen to be only a matter of definition [43]. Finally, the CT contributions are contained in the following Lagrangian piece extracted from (5) – for the normalization – and (1):

$$\mathcal{L}_{\gamma\pi^+\pi^-P^0} = -i\frac{e}{8\pi^2 f_\pi^3} \epsilon^{\mu\nu\alpha\beta} A_\mu \partial_\nu \pi^+ \partial_\alpha \pi^- \quad (16)$$

$$\times \left[\partial_\beta \pi^0 + \frac{1}{\sqrt{3}} \partial_\beta \eta_8 + x \sqrt{\frac{2}{3}} \partial_\beta \eta_0 \right] .$$

Changing from η_8, η_0 to η, η' is performed by a rotation involving the (wave-function) mixing angle:

$$\begin{bmatrix} \eta \\ \eta' \end{bmatrix} = \begin{bmatrix} \cos \theta_P & -\sin \theta_P \\ \sin \theta_P & \cos \theta_P \end{bmatrix} \begin{bmatrix} \eta_8 \\ \eta_0 \end{bmatrix} \quad (17)$$

There is, obviously, no loss of generality in introducing this definition and, thus, the physical parameter θ_P which has to be fixed or fitted.

For all expressions in this section, the fields which occur are the renormalized ones. It should already be noted that all basic Lagrangian pieces involved in the considered η/η' decays do not depend at leading order on the SU(3) breaking mechanism (the parameter $z = [f_K/f_\pi]^2$ already met), at least in the limit of isospin symmetry where we are concerned with. However SU(3) symmetry breaking is hidden inside θ_P (see (10)).

6.2 Amplitudes and chiral limit properties

With the information given just above, it is an easy task to compute the amplitudes for the η/η' decays considered. One finds

$$T(X \rightarrow \pi^+ \pi^- \gamma) \quad (18)$$

$$= c_X \frac{ie}{8\sqrt{3}\pi^2 f_\pi^3} \left[1 + \frac{3m_\rho^2}{D_\rho(s)} \right] \epsilon^{\mu\nu\alpha\beta} \epsilon_\mu k_\nu p_\alpha^+ p_\beta^- ,$$

using an obvious notation, with $X = \eta, \eta'$, $m_\rho^2 = ag^2 f_\pi^2$ and s being the dipion invariant mass. The c_X are given by

$$c_\eta = [\cos \theta_P - x\sqrt{2} \sin \theta_P] ,$$

$$c_{\eta'} = [\sin \theta_P + x\sqrt{2} \cos \theta_P] . \quad (19)$$

Finally $D_\rho(s)$ is the inverse ρ propagator which can be written [43]

$$D_\rho(s) = s - m_\rho^2 - \Pi_{\rho\rho}(s) , \quad (20)$$

in terms of the already defined (KSFR) ρ mass and of the ρ self-mass. The occurrence of $\Pi_{\rho\rho}(s)$ permits one to move the ρ pole off from the physical region [43, 61]. For

the present purpose, one has only to stress that the ρ self-mass can be chosen rigorously such that $\Pi_{\rho\rho}(0) = 0$ as expected from current conservation [63].

Going to the chiral limit, (18) is nothing but the second one of (2) and has for coefficients

$$E'_\eta(0) = -\frac{ie}{4\sqrt{3}\pi^2 f_\pi^3} [\cos \theta_P - x\sqrt{2} \sin \theta_P] ,$$

$$E'_{\eta'}(0) = -\frac{ie}{4\sqrt{3}\pi^2 f_\pi^3} [\sin \theta_P + x\sqrt{2} \cos \theta_P] . \quad (21)$$

These relations clearly meet the expectations of current algebra; they could not be derived exactly if $\Pi_{\rho\rho}(0) \neq 0$. The single symmetry breaking parameter occurring manifestly is x which essentially measures departs from nonet symmetry.

It should be noted that there is no obvious connection between the way symmetry breaking occurs for the box anomaly (see (21)) and for the triangle anomaly (see (11)) within the broken HLS model. It is worth recalling once more that the symmetry breaking scheme defined in Sect. 4 was shown [32] to match perfectly all expectations of EChPT collected in [2, 3, 50] and that no further piece has been added in order to derive (21).

Therefore, the second assumption which underlies the traditional way of breaking symmetries for this set of equations (see the discussion after (3)) is also not met by the BKY breaking scheme [32, 39, 40].

Equations (21) are also interesting in other aspects: In order to recover the values expected for both $E'_X(0)$, the VMD (i.e. resonant) contribution happens to be 3 times larger than the contact term (CT) contribution and carries an opposite sign; this was expected when building the anomalous HLS Lagrangian (5).

Equations (18) also show that fitting the η/η' invariant-mass spectra with a constant term interfering with a resonant term is indeed legitimate. However, it is also clear that the value of this constant is *not* the value of the full amplitude at the origin and thus carries only a part of the box anomaly value.

The triangle and box anomaly expressions in the broken HLS model are summarized by (11) and (21). We know from previous works [32, 41] that the experimental data support this in the triangle anomaly sector (AVP and $\eta/\eta' \rightarrow \gamma\gamma$); the real issue is to test its validity in processes where box anomalies are expected to occur.

6.3 The $\gamma\pi^+\pi^-\pi^0$ amplitude

Even if outside the main stream of this paper, it is interesting to give the amplitude for the $\gamma\pi^+\pi^-\pi^0$ anomalous coupling for which the effects of radiative corrections have recently been considered [64]. Using (1) and (14) above, together with the piece analogous to (15) for ρ^\pm which can be found in [40], one gets

$$T(\gamma \rightarrow \pi^+ \pi^- \pi^0) = A(s, t, u) \epsilon^{\mu\nu\alpha\beta} \epsilon_\mu p_\nu^+ p_\alpha^- p_\beta^0 , \quad (22)$$

with

$$A(s, t, u) = \frac{e}{8\pi^2 f_\pi^3} \left[1 + \frac{m_\rho^2}{D_\rho(s)} + \frac{m_\rho^2}{D_\rho(t)} + \frac{m_\rho^2}{D_\rho(u)} \right], \quad (23)$$

where $m_\rho^2 = ag^2 f_\pi^2$ and D_ρ is given by (20) with the appropriate permutation of the argument s to t and u . In this case, the symmetry breaking mechanism we have defined has no influence. The momentum dependence of this expression differs from the known ones (written in (39) and (40) in [8]) by its taking into account the ρ self-energy (see (20)). It gives the expected value ($-ie/4\pi^2 f_\pi^3$) at $s = t = u = 0$ and is worth to be checked on forthcoming experimental data [65]. It might also be extracted from $e^+e^- \rightarrow \pi^+\pi^-\pi^0$ annihilation with data covering the low invariant-mass region.

6.4 Invariant-mass spectra and the box anomaly

From the amplitude in (18), one derives the decay width:

$$\frac{d\Gamma(X \rightarrow \pi^+\pi^-\gamma)}{d\sqrt{s}} = \frac{c_X^2}{36} \frac{\alpha}{[2\pi f_\pi]^6} \left| 1 + \frac{3m_\rho^2}{D_\rho(s)} \right|^2 k_\gamma^3 q_\pi^3, \quad (24)$$

for each of the η and η' mesons. We have defined $k_\gamma = (m_X^2 - s)/2m_X$, the photon momentum in the X rest frame and $q_\pi = \sqrt{s - 4m_\pi^2}/2$, the pion momentum in the dipion rest frame.

The contact term generated by the second piece in (5), is represented in (24) by the number 1 inside the modulus squared. On the other hand, as the normalization of the VMD contribution can be fixed [41,42] at the appropriate value by only normalizing to the $P\gamma\gamma$ amplitude in (13), checking the effect of this contact term by switching on/off this “1” in (24) is indeed meaningful. In this way, one can address the experimental relevance of (5).

Equation (24) is interesting in many regards.

(1) The shape of the invariant-mass spectra depends on the η/η' meson properties only through a kinematical factor (k_γ^3). Therefore, the shape of the invariant-mass spectra does not carry any *manifest* information on the box anomaly constants c_X .

(2) The lineshape of the invariant-mass spectra in η/η' decays depends only on ρ meson properties. However, the way this dependence occurs in η/η' decays is different from the one in the pion form factor [43], as the dressing of the ρ - γ transition amplitude $\Pi_{\rho\gamma}(s)$ plays no role in the η/η' decays.

(3) All information on the value of c_η and $c_{\eta'}$ is carried by the partial width itself. It can be algebraically derived if $D_\rho(s)$ is known reliably from another source.

In order to perform a search for the box anomaly, one needs a function $D_\rho(s)$ accurately determined between the two-pion threshold and the ϕ mass. In the physical region involved in η/η' decays, all coupled channels allowed by the HLS model contribute at one-loop order [43]. However,

except for $\pi^+\pi^-$, each provides⁷ only logarithms, beside their influence on the subtraction polynomial hidden inside the ρ^0 self-mass $\Pi_{\rho\rho}(s)$. This is their major effect, and thus neglecting these loops while still considering a subtraction polynomial of the appropriate degree is certainly motivated.

Reduced to only its coupling to $\pi^+\pi^-$ (with or without accounting for kaon pairs), the ρ propagator used here contributes to providing a fairly accurate numerical determination of the pion form factor both in modulus [43,61] and in phase [43] up to the ϕ mass. Therefore, for the purpose of studying the box anomaly, there no point in going beyond contributions from only the non-anomalous HLS Lagrangian. In this case, the ρ self-energy can be written

$$\Pi_{\rho\rho}(s) = g_{\rho\pi\pi}^2 \left[\ell_\pi(s) + \frac{1}{2z^2} \ell_K(s) \right], \quad (25)$$

where $g_{\rho\pi\pi} = ag/2$, while z has already been defined. We have denoted by $\ell_\pi(s)$ and $\ell_K(s)$ the pion and kaon loops amputated from their couplings to external legs (we neglect the mass difference between K^\pm and K^0); these are given in closed form in [42].

These loops should be subtracted at least twice in order to make convergent the dispersion integrals which define them as analytic functions; this gives rise to a first degree polynomial $P_\rho(s)$ with arbitrary coefficients to be determined by imposing explicit conditions or by a fit. However, as noted just above, anomalous loops force one to perform, at least, three subtractions [42,43], which modifies the arbitrary polynomial $P_\rho(s)$ to (at least) second degree. This is the reason why $P_\rho(s)$ will be assumed to be of second degree, even if one limits oneself to pion and kaon loops. This does not increase our parameter freedom, as will be seen shortly.

6.5 External numerical information

From what can be seen above, the condition $P_\rho(0) = 0$ on the subtraction polynomial is certainly desirable; otherwise the current algebra expectations could not be derived exactly; additionally, this condition ensures masslessness of the photon after dressing by pion and kaon loops. There thus remain two subtraction constants to be determined or chosen; we shall fix them from the fit performed [43] on the pion form factor from threshold to the ϕ mass. Denoting by $\overline{\Pi}_{\rho\rho}(s)$ the ρ self-energy subtracted three times [42], we have

$$\Pi_{\rho\rho}(s) = \overline{\Pi}_{\rho\rho}(s) + e_1 s + e_2 s^2. \quad (26)$$

On the other hand, we can also fix the HLS parameters a , g (and thus m_ρ) and x to their values fitted in radiative

⁷ And, to some extent, except also for the $\omega\pi^0$ channel in the η' decay; however, the neglected effect is concentrated in the region above 917 MeV, very close to the phase space boundary for η' decay and far beyond in the η decay

Table 1. Parameter values for a , g , x , z fixed from a global fit to $VP\gamma$ and $V \rightarrow e^+e^-$ decay modes [41,42,55]; e_1 and e_2 are fixed from a fit [43] to the pion form factor including only $\pi\pi$ and $K\bar{K}$ as channels coupling to ρ

Parameter	Value
a	2.51 ± 0.03
g	5.65 ± 0.02
x	0.90 ± 0.02
$z = [f_K/f_\pi]^2$	1.51 ± 0.02
e_1	0.222 ± 0.011
e_2	$-1.203 \pm 0.017 \text{ GeV}^{-2}$

Table 2. Partial widths for $\eta/\eta' \rightarrow \gamma\gamma$ as predicted using (11) with parameter values as coming from a global (HLS) fit to only $VP\gamma$ decay modes of light mesons [32]

Parameter	PDG 2002	Prediction	Significance ($n \sigma$)
$\eta \rightarrow \gamma\gamma$ (keV)	0.46 ± 0.04	0.46 ± 0.03	0.0 σ
$\eta' \rightarrow \gamma\gamma$ (keV)	4.29 ± 0.15	4.41 ± 0.23	0.4 σ

and leptonic decays⁸ [41, 42]. Knowing z and x , one can derive the value for θ_P from (10). The values for e_1 and e_2 are fixed from an appropriate fit to the pion form factor [43], where the parameters a , g and x are fixed consistently with AVP and $(\omega/\phi)e^+e^-$ modes.

As we restrict the ρ coupling to only the $\pi^+\pi^-$ and $K\bar{K}$ channels, these values for e_1 and e_2 are certainly correlated with the chosen values for a and g ; they are not affected numerically by the value for x .

The values for these parameters are gathered in Table 1. As these parameters are supposed to be universal in the realm of the HLS model, one can fix their values from a fit to the data independent of the $\eta/\eta' \rightarrow \pi^+\pi^-\gamma$ decay modes. It is indeed the case for the $VP\gamma$ or the Ve^+e^- decay modes and for the pion form factor. As commented on above, these fit values correspond to a very good fit quality for the corresponding data. For instance, they allow one to *predict* [32] the two-photon decay widths as is clear in Table 2.

Choosing the ρ propagator as it comes out of the HLS fit to the pion form factor [43] is also fairly legitimate, as this ρ propagator should also be valid anywhere within the HLS framework. As stated above, we consider for clarity only the case where the only open channels are $\pi\pi$ and $K\bar{K}$. We have, nevertheless, checked that changing to various open channel subsets coupling to the ρ meson (as done in [43] for the pion form factor), with correspondingly changing e_1 and e_2 to their fit values, does not produce any significant modification to the results presented below.

To summarize, self-consistency implies that we can fix all parameters and functions from their most reliable fit values and expressions, provided the data set is indepen-

⁸ Actually, the values for g and x are determined almost solely by the AVP radiative decays; the value for a is a consequence of these on the $V \rightarrow e^+e^-$ decay modes, but mostly the ω and ϕ leptonic decays

dent of the η/η' decays considered here. This independent data sample covers $VP\gamma$ and Ve^+e^- couplings [32, 41, 42] and the pion form factor [43]. It then follows that all information related with the box anomalies can be *predicted* without any parameter freedom.

7 Predictions for $\eta/\eta' \rightarrow \pi^+\pi^-\gamma$ decays

In this section, we examine the predictions derived for the $\eta/\eta' \rightarrow \pi^+\pi^-\gamma$ decay modes for the partial widths and dipion invariant-mass distributions.

7.1 Partial widths, experimental values and predictions

Using (24) and the numerical (and functional) information given in the previous subsection, it is easy to check that we can write

$$\Gamma(X \rightarrow \pi^+\pi^-\gamma) = A_X c_X^2, \quad (27)$$

where

$$A_X = \frac{1}{36} \frac{\alpha}{[2\pi f_\pi]^6} \int_{2m_\pi}^{m_X} \left| 1 + \frac{3m_\rho^2}{D_\rho(s)} \right|^2 k_\gamma^3 q_\pi^3 d\sqrt{s},$$

$$X = \eta, \eta' \quad . \quad (28)$$

This integration can be done by Monte Carlo techniques and gives

$$A_\eta = 38.25 \pm 1.07 \text{ eV}, \quad A_{\eta'} = 42.16 \pm 3.00 \text{ keV} \quad . \quad (29)$$

As further information, one should note that these integrals are not affected by the value for x . Using the parameter values given in Table 1, (19) and (10), one can *compute* the partial widths and get the results collected in Table 3. We have performed the computation by switching on/off the contact term contribution.⁹ We stress again that all results presented in this section do not depend on any free parameter and thus are *predictions* relying on the rest of the HLS phenomenology.

From Table 3, one clearly sees that the *predicted* partial width for η' is not really sensitive to the presence of the contact term. This can be well understood as, indeed, the value for $A_{\eta'}$ is sharply dominated by the ρ peak contribution provided by the VVP Lagrangian term and the magnitude of the contact term is comparatively small.

In contrast, the *predicted* partial width for η is much more sensitive to the contact term because this contribution has only to compete with the low mass tail of the ρ distribution; the bulk of the resonance contribution is indeed sharply suppressed because the available phase space is small and located far outside the ρ peak.

Therefore, one can already conclude from Table 3 that the η/η' partial widths values provide strong evidence in

⁹ When switching off the contact term in (28), the numbers in (29) become $A_\eta = 57.51 \pm 4.01 \text{ eV}$ and $A_{\eta'} = 49.60 \pm 2.98 \text{ keV}$, which is already conclusive

Table 3. η/η' Partial widths as predicted by the HLS model when switching on/off the box anomaly contribution. The significance is computed using an error obtained by adding in quadrature the experimental error and the relevant model error computed by Monte Carlo sampling (using information in Table 1)

Decay	PDG 2002	Prediction with box anomaly	Prediction without box anomaly
$\eta \rightarrow \pi^+\pi^-\gamma$ (eV)	55 ± 5	56.3 ± 1.7	100.9 ± 2.8
Significance ($n \sigma$)		0.25σ	8σ
$\eta' \rightarrow \pi^+\pi^-\gamma$ (keV)	60 ± 5	48.9 ± 3.9	57.5 ± 4.0
Significance ($n \sigma$)		1.75σ	0.39σ

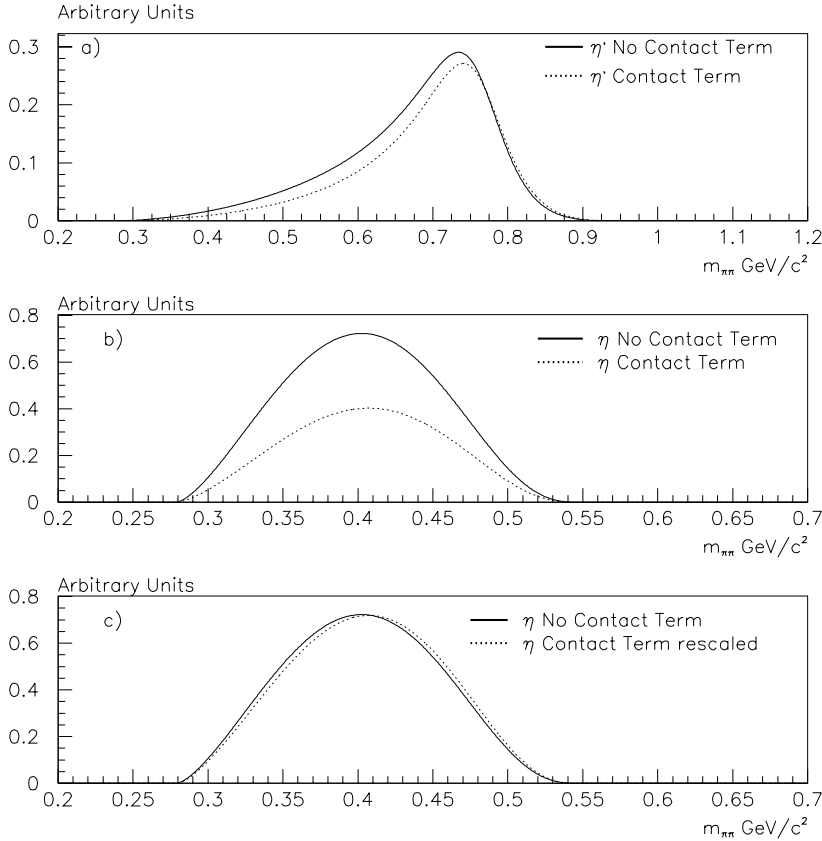


Fig. 1. Predicted shapes for η' (top) and η (mid) distributions as functions of the dipion invariant mass. Full line histograms correspond to having the contact term in the amplitude, dotted line histograms correspond to removing the contact term from the amplitude. All other numerical parameters are at the same values (see Table 1). In the bottom figure, we plot the prediction when accounting for the contact term (rescaled) superimposed with the prediction derived by removing this contribution

favor of the box anomaly. Unexpectedly, this evidence is provided by the η partial width alone. Additionally, the values *predicted* for the box anomaly constants $c_\eta \simeq 1.21$ and $c_{\eta'} \simeq 1.07$ from the rest of the HLS phenomenology fit nicely the η/η' partial widths, which means, for instance, consistency with $\theta_P = -10.30^\circ \pm 0.20^\circ$.

Together with the results predicted for two-photon decay widths of the η/η' system, this also gives strong support to the extended BKY breaking scheme summarized in Sect. 4 and to (11) and (21) for the amplitude expressions at the chiral limit.

7.2 Invariant-mass spectra with/without the contact term

The shape of the dipion invariant-mass distributions are given in Fig. 1, top for η' , middle for η . These are propor-

tional to the yields (up to acceptance/efficiency effects). The distributions are displayed with having switched on/off the contact term; in these two figures, the relative magnitude of the twin distributions is respected.

Looking at the η distributions, one clearly understands the width results given in Table 3, as the integrals corresponding to box anomaly on/off are clearly very different (actually by a factor of about 2).

In the case of the η meson, lineshape differences between the case when the contact term is activated and when it is dropped are tiny as illustrated by Fig. 1, bottom. In this figure, one displays the distribution obtained by removing the contact term and the one derived by activating it, after rescaling it by $\simeq 1.8$.

The lineshape, in the case of the η' , shows that the peak location when accounting for the contact term is slightly at higher mass ($6 \div 8$ MeV) compared to the case when this

(CT) contribution is cancelled. However, the main effect is that yields below the ρ peak location are somewhat suppressed because of the contact term.

In this sort of situation, if one performs a fit of an η' spectrum affected by CT with only a resonance contribution and lets free the resonance parameters, the shape will be distorted. Indeed, in order to reasonably average the rising wing of the ρ distribution, the peak has to be shifted to a higher mass and therefore the observed mass must be larger. This is a mechanical effect connected with the minimization of a χ^2 for any appropriate function of one variable. We come back to this point when comparing with the experimental data.

8 Experimental data on $\eta/\eta' \rightarrow \pi^+\pi^-\gamma$ decays

There are several sets of data available for the dipion mass spectrum of the η' meson. Most of them have been published only as figures [12–17]. For these, however, it happens that the information given in the body of the articles provides enough information in order to recover the yields and derive the acceptance/efficiency function; the redundancy of the information is fortunately such that consistency checks and cross checks can be performed which validate the outcome of the procedure. This is described in detail in Sect. 4 of [33] together with the peculiarities of each of these data sets.

Other spectra were available directly to us [18] or as Ph.D. theses [19–22] published only as preprints. Here also the relevant information was either directly available or could be reconstructed accurately, as for the references quoted above. One should note that the data of [21] supersede the ARGUS results published in [14].

These former data samples carry widely spread statistics; 474 events for the oldest data set [12], 130 events from TASSO [13], 795 events from ARGUS [14] updated three years later to 2626 [21], 321 events in the TPC- $\gamma\gamma$ sample [15], 195 events in the PLUTO data set [19], 586 in the CELLO data set [22], 401 for the data set of WA76 collected using the Omega Prime Spectrometer at the CERN SPS [18] and, finally, 2491 (after acceptance corrections) for the experiment performed at Serpukhov using the LEPton F facility [17].

The method used to extract the dipion invariant-mass spectra from the data is of special concern. These were derived from the data samples just listed in the following way: for each bin of dipion invariant mass, one plots the $\pi^+\pi^-\gamma$ invariant-mass spectrum and fits with a Gaussian (plus a polynomial background) the number of η' it contains. In this way, one gets rid to a large extent of the precise background¹⁰ parametrization, as the signal is a narrow Gaussian peak dominated by the experimental resolution.

¹⁰ We have to make assumptions on the background shape across some small $\pi^+\pi^-\gamma$ mass interval while the signal is a narrow Gaussian (typically 20 to 30 MeV for its standard deviation). This is certainly much safer than assumptions on the background shape over a 1 GeV invariant-mass interval with on top of this a signal as broad as a ρ distribution

Performing this way, spectra appear without any background and the influence of this in the data sets only is reflected in the magnitude of the errors on the yields per bin. It should be stressed that this extraction method is obviously independent of any assumption on the lineshape of the underlying ρ invariant-mass distribution.

For the data samples of [17–19], the acceptance/efficiency function was directly known, but without information on its uncertainties. As the spectra of [18, 19] carry small statistics, statistical errors are dominant and errors on the acceptance/efficiency function can be neglected. For the data sample of [17], the acceptance/efficiency function is provided as a curve (see Fig. 3 therein); as no information is reported about uncertainties affecting this function, these cannot be accounted for when folding in this function with any model distribution.

For the other data samples reviewed above, uncertainties on the acceptance/efficiency functions are also unknown, as these can only be derived by unfolding it from the fitting distribution. This was always provided as a product of a well-defined model function for the decay with this acceptance/efficiency function. This is also of little importance for all data sets dominated by statistical errors, but it also affects the large statistical sample of ARGUS we shall examine [21].

Neglecting this source of uncertainties when computing model errors certainly biases χ^2 estimates towards larger values (and smaller probabilities). However, it should not spoil qualitatively the model descriptions.

The sample of MarkII [16] is also significant ($\simeq 1200$ events); however, the mass spectrum derived from this has been obtained in a different way: Selecting the events in some mass interval around the η' mass in the *global* $\pi^+\pi^-\gamma$ invariant-mass spectrum, the corresponding events are plotted in bins of $\pi^+\pi^-$ invariant mass. This spectrum is then described as a superposition of a ρ mass distribution plus some background, and a global fit to this spectrum provides the signal (ρ) and background populations inside each bin. Therefore this method assumes an accurate knowledge of all phenomena contributing to the background (and of its parametrization); it also relies on the way the ρ lineshape is parametrized. This is also, basically, the method used to study the η' mass distribution performed by the L3 Collaboration [24] on a sample of 2123 ± 53 events; this will be specifically discussed at the appropriate place below, as it is the latest published data sample.

Some other papers published spectra without background subtraction (namely [20, 62] which actually contain the same data). In order to use these, one would have to model the background without any motivated knowledge of the data set and detector properties¹¹; therefore, this MarkII spectrum will not be examined here. This lack of background subtraction is also the reason why the spectrum published by the L3 Collaboration is also not kept.

¹¹ Indeed, beside extracting the yields, one needs to estimate the acceptance/efficiency function which might well be different for signal and background events

Finally, the most reliable spectrum for the η' decay is the one collected by the Crystal Barrel Collaboration [23] which is also, by far, the largest data sample (7392 events). This spectrum has been constructed using the method described at the beginning of this section; therefore, it is independent of any assumption on the underlying ρ invariant-mass distribution and, thus, is certainly free from any prejudice or bias. Additionally, this data sample is certainly the most secure to be used as uncertainties on acceptance and efficiencies are already included into yield errors and, thus, a model comparison can be performed directly and reliably.

The corresponding spectra for the η decay have been derived from $\pi p \rightarrow \eta n$ data collected long ago by two experiments [10, 11]; the published data are already background subtracted. They both carry large statistics (7250 for [10] and 18150 for [11]). The relevant results have been published only as figures. Yields per bin can be read off from these figures without any difficulty together with their errors.

In [10], the acceptance/efficiency function is provided directly and also folded in with a well-defined model function. It is given superimposed to the case when the analysis is performed with a simple gauge-invariant phase-space matrix element and with a ρ dominant one. The two corresponding acceptance/efficiency functions are conflicting, essentially in the region $k_\gamma = 90 \div 110$ MeV. However, this seems to reflect their dependence upon the angular distributions. It is therefore worth using the functional information associated with the ρ dominant matrix element.

For the data of Layter et al. [11], the acceptance/efficiency function is not shown and should be unfolded from the theoretical ρ (and phase-space) distribution(s). This information can be extracted with some reliability; in contrast with [10], this yields a function extracted from the ρ distribution very close from those extracted from the simple phase space distribution. Actually, this data set should be considered with some care as extracting the acceptance/efficiency function can only be performed by making some assumption on the ρ mass actually used in this paper [11]. We have conservatively assumed that Layter et al. [11] used the same ρ mass as Gormley et al. [10], namely $m_\rho = 765$ MeV; this assumption is crucial and cannot be ascertained. This makes more secure the information derived from the Gormley spectrum.

Finally, for both η spectra, it is impossible to restore the accuracy on the acceptance/efficiency function. These will be considered negligible in the present study.

9 Experimental data versus predictions for η/η' spectra

As seen in Sect. 6.4, the HLS model provides definite spectra for both η/η' invariant-mass distributions. These depend on parameters which can be fixed independently of the $\eta/\eta' \rightarrow \pi^+\pi^-\gamma$ spectra, like a , g , x (see Sect. 6.5), and of the ρ propagator which is fitted elsewhere [43] with parameters values as determined in these fits (see (26) and Table 1). The model fairly well predicts the absolute

magnitude (the integral) of each spectrum as illustrated in Table 3. In this section, we focus on comparing the *predicted* lineshapes derived from the model (24) with the data listed in Sect. 8.

As all data considered are binned, we have integrated the predicted function (24) (or (28)) over the bin size and normalized this function to the integral of the experimental distribution. When relevant (i.e. all spectra except for the one of the Crystal Barrel [23]), the model function was folded in with the acceptance/efficiency function derived for each of the above data samples.

The results are displayed in Figs. 2 to 4. One should note that all η' spectra are given as functions of the dipion invariant mass, while the η spectra are given as functions of the photon momentum in the η rest frame.

In these figures, together with the specific experimental spectrum, we show the predicted curve (computed just as defined above) when keeping the contact term (full curve) and the one derived by dropping this contribution (dashed curve). These two cases will be referred to as respectively CT and NCT. In these figures, we give the χ^2 corresponding to these two solutions under the form $\chi^2(\text{CT})/\chi^2(\text{NCT})$. The number of degrees of freedom can be easily read off from the spectra as this is exactly the number of bins of the experimental histogram.

The curves shown have been computed at the central values of the parameters as given in Table 1. The χ^2 have been computed by folding in the experimental error in each bin with a model error also computed bin per bin. These model errors have been computed by sampling the parameters around their central values with standard deviations given by their quoted errors (see Table 1). Except for the Crystal Barrel case [23], where it is irrelevant, uncertainties on the acceptance/efficiency functions are not (cannot be) accounted for. The curves shown are actually histograms which have been smoothed automatically by the `hbook/paw` package.

Examination of Figs. 2 to 4 is quite interesting. First of all, the spectrum from TPC- $\gamma\gamma$ is clearly singular in being far away from the predictions, indicating that something was not well controlled when extracting it from the data. All others match well, or quite well, the predictions; this clearly gives support to the model developed in the previous sections and to the relevance of the parameters given in Table 1.

In terms of probabilities (reflected by the χ^2/dof values given in the figures), the oldest data set of [12] gives comparable probabilities to either of the CT/NCT assumptions, while maybe slightly preferring the NCT assumption. CT/NCT descriptions are practically equivalent for the ARGUS [21] and WA76 [18] spectra, while nevertheless slightly favoring the CT assumption.

The relatively low statistics spectra provided by TASSO [13] (χ^2 ratio of 0.6 in favor of the CT assumption), CELLO [22] (0.7) and PLUTO [19] (0.7) somewhat prefer the CT assumption.

Finally, the two largest statistics experiments Lepton F [17] and Crystal Barrel [23] sharply favor both the CT

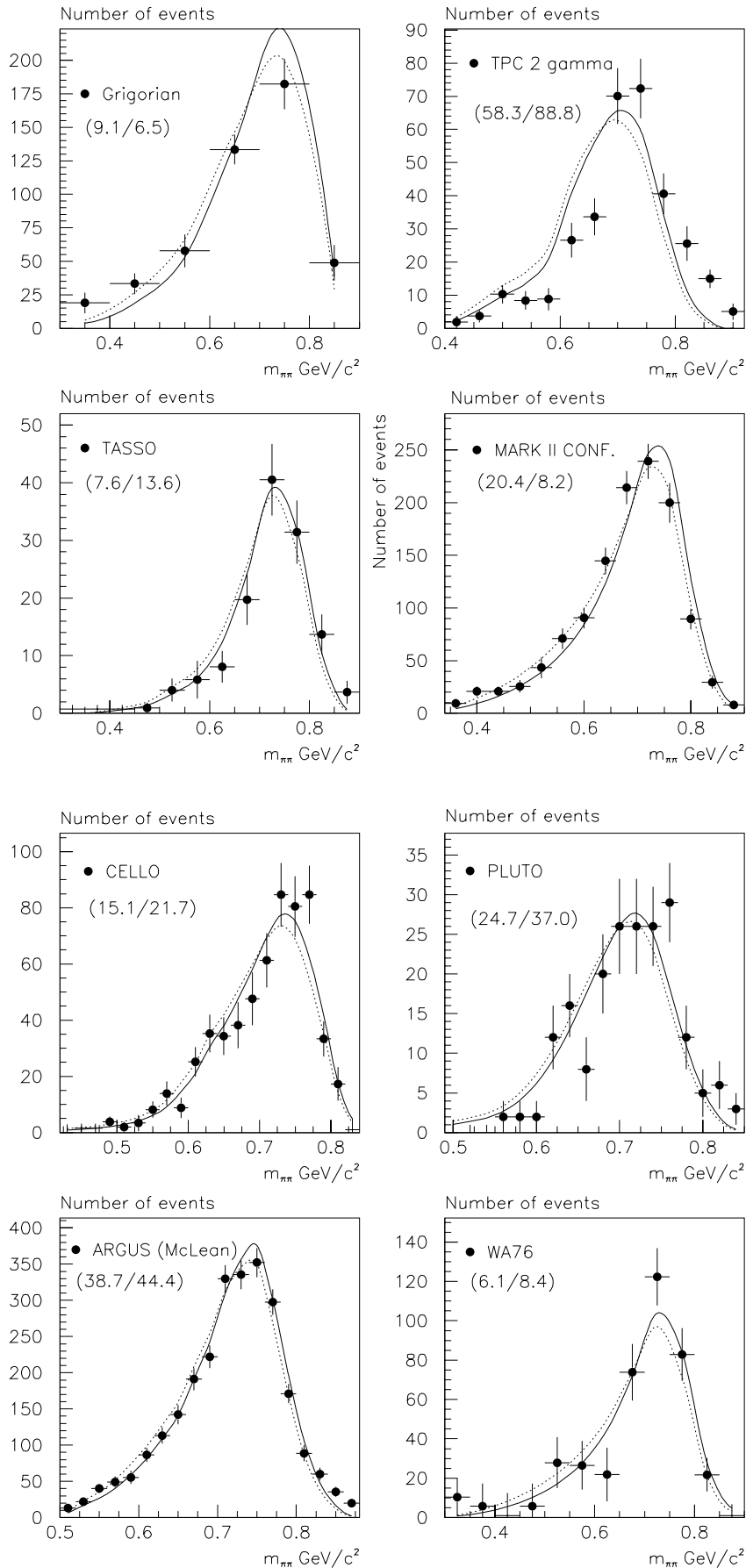


Fig. 2. Invariant dipion mass distributions for η' decay. Experimental data sets with the predicted distributions are shown without the contact term (dashed curve) and with this contribution activated (full curve). The numbers given are $\chi^2(\text{contact term})/\chi^2(\text{no contact term})$ for the lineshapes only

Fig. 3. Invariant dipion mass distributions for η' decay. Experimental data sets with the predicted distributions are shown without the contact term (dashed curve) and with this contribution activated (full curve). The numbers given are $\chi^2(\text{contact term})/\chi^2(\text{no contact term})$ for the lineshapes only

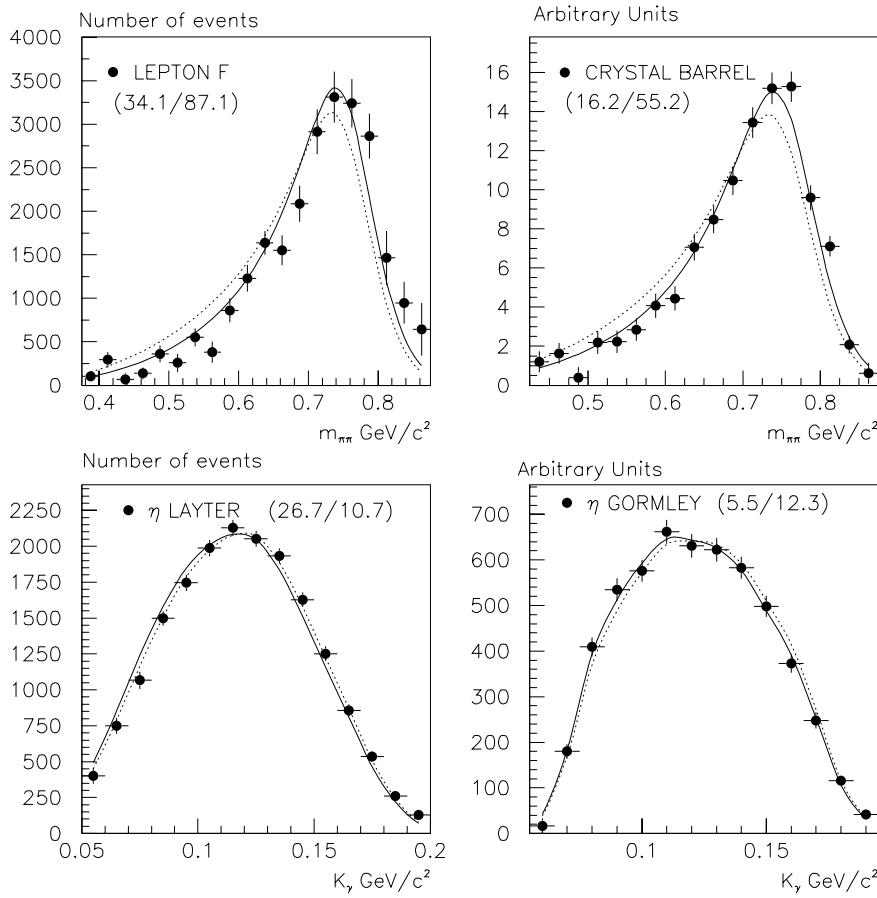


Fig. 4. Invariant dipion mass distributions for η' decay and the single η decay (as a function of the photon momentum in the η rest frame). Experimental data sets with the predicted distributions are shown without the contact term (dashed curve) and with this contribution activated (full curve). The numbers given are $\chi^2(\text{contact term})/\chi^2(\text{no contact term})$ for the lineshapes only

assumption against NCT; the χ^2 distance is indeed better by more than a factor of 2.

To be more precise the Lepton F spectrum¹² gives a 3% probability to the CT assumption and a $2 \cdot 10^{-8}$ probability to the NCT assumption. These relatively low probabilities should be related with the lack of information on the acceptance/efficiency function which affects in the same manner both solutions. Accounting for the corresponding errors would certainly increase both probabilities but hardly switch their ordering.

The corresponding probabilities for the Crystal Barrel data set are respectively 57.8% and 0.1%; these values are certainly realistic as the model errors are reasonably well accounted for.

Among these two data sets which could be used as a reference, the Crystal Barrel data (available in a directly usable form [23]) should clearly be preferred, as systematics are better controlled all along the invariant-mass range. It also carries, by far, the largest statistics.

From χ^2 values, the shape of the η spectrum from Layter et al. [11] seems in better agreement with the NCT

assumption (77% probability) than with the CT assumption (3% probability).

In contrast, the description of the η spectrum from Gormley et al. [10] is simply perfect and corresponds to respectively 97.7% probability for the CT assumption and to 58.2% probability for the NCT assumption; this reflects better the remark following from Fig. 1 (bottom) that these lineshapes are very close together. The χ^2 values, however, indicate that the geometrical distance ($\simeq \sqrt{\chi^2}$) of this spectrum to the CT solution is significantly smaller than those to NCT.

Figure 5 gives the same information as in Fig. 4 but enlarged and binned. Here one sees that a third of the χ^2 for the Layter spectrum [11] comes from only the bin covering the momentum interval $60 \div 80 \text{ MeV}/c$. Compared to the same result for the Gormley spectrum [10], the Layter spectrum looks a little bit skewed. It is, however, impossible to decide whether this comes from systematics affecting the acceptance/efficiency function as this (skewed) shape happens to match nicely the NCT assumption.¹³

¹² The eight lowest mass points of this spectrum contribute severely to the χ^2 for both (CT/NCT) assumptions. On the other hand, the sharp drop in acceptance [17] at large $m_{\pi\pi}$ might have been difficult to estimate reliably. Qualitatively, however, the clear preference of this distribution for the CT assumption is obvious

¹³ This skewness might have been magnified unwillingly by the choice of the m_ρ value we performed in order to extract the acceptance/efficiency function for the Layter spectrum. Any underestimation of this input m_ρ value contributes to the skewness of this distribution. We are responsible for this uncertainty, but we did not find an unbiased way out

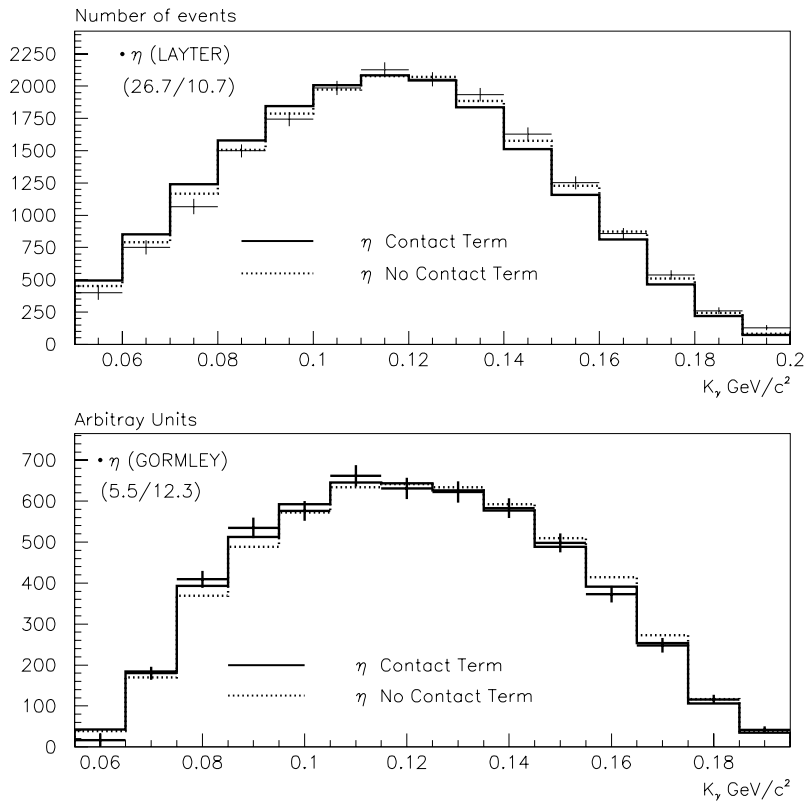


Fig. 5. Photon momentum distribution in η decay experimental data are from Layer et al. [11] (top), and Gormley et al. [10] (bottom); experimental data sets with the predicted distributions are shown without the contact term (dashed curve) and with this contribution activated (full curve). The numbers given are $\chi^2(\text{contact term})/\chi^2(\text{no contact term})$ for the lineshapes only

However, the $\eta \rightarrow \pi^+\pi^-\gamma$ partial width alone [9], certainly more secure information, and the Gormley spectrum undoubtedly favor the CT assumption against the NCT one. These two aspects have to be balanced in a global fit accounting for lineshapes and partial widths.

10 A global fit to η/η' spectra and widths

We have compared the data (lineshapes and partial widths) with the predictions of our model fed with numerical and functional information coming from the rest of the phenomenology accessible to the HLS framework, without any parameter freedom. The results obtained in Sects. 7 and 9 considered together indicate that the model is valid and favors the contact term as a physically motivated contribution to decay processes. We recall that this contact term is *not* a free parameter, as amply discussed above.

In view of this, it looks worth performing a simultaneous fit of the η data sets with some accurate η' spectrum; for reasons explained above, it is certainly worth choosing the Crystal Barrel spectrum. As a clear conclusion should take into account all aspects of the available experimental information, partial widths have been fed into the χ^2 to be minimized.

In order to perform this fit one needs to release some of the parameters fixed as in Table 1; as the main information for the present purpose is the peak location, it looks worth releasing the parameters named e_1 and e_2 , which mostly influence the ρ peak location. Comparing the values re-

turned from this fit to the corresponding values originally extracted from fitting the pion form factor could contribute to clarify the conclusion, as one can consider the ρ propagator as a universal function, as valid for $F_\pi(s)$ as for the η/η' spectra.

Indeed, we know that, in the pion form factor, the subtraction polynomials of $\Pi_{\rho\rho}(s)$ and $\Pi_{\rho\gamma}(s)$ are somewhat competing and that some (small) correlation among the corresponding polynomials exists [43]; it is therefore motivating to attempt freeing e_1 and e_2 as these correlations could have spoiled their central values by some (certainly) small amount. However, the parameter values returned from the fit must not be inconsistent with their partners derived from the fit to the pion form factor only.¹⁴

On the other hand, the other parameter values in Table 1 describing fairly well the full set of $V \rightarrow P\gamma$ and $P \rightarrow V\gamma$ decays would hardly accommodate a significant change of their values without failing to fit the $VP\gamma$ processes.

In order to avoid too much correlations which can hide the clarity in the conclusions, we shall test separately the CT and the NCT assumptions. Indeed, as the HLS model predicts the magnitude of the constant contact term (if any), it seems enough to check its precise relevance and no attempt will be made to fit its value. Finally, for the

¹⁴ This actually means that a further test could be a simultaneous fit, within a consistent framework, of the pion form factor and of the relevant η/η' decay information. One does not expect a surprise nor hard difficulties from such an attempt; the present work indicates that this should not provide more insight than a global probability

Table 4. Simultaneous fits of the η/η' distributions from [11, 23] on the one hand, and from [10, 23] on the other hand. CT stand for the “contact terms” generated by the box part of the WZW Lagrangian (see (5)). The values for e_1 and e_2 quoted in “No fit” entries are taken from Table 1 and not varied from their central values. The “P.W.” entries are the central values for the η and η' partial widths in the appropriate units; the recommended values for these [9] are given in Table 3

Layter [11]					
	e_1	e_2 (GeV ⁻²)	χ^2/dof (Prob.)	η P.W. (eV)	η' P.W. (keV)
CT + No fit	0.222 ± 0.011	-1.203 ± 0.017	37.88/35 (34%)	56.3	48.9
CT + Fit	$0.339^{+0.105}_{-0.056}$	$-1.395^{+0.143}_{-0.160}$	35.16/33 (36.6%)	53.3	46.2
No CT + No fit	0.222 ± 0.011	-1.203 ± 0.017	140.65/35 (0%)	100.9	57.5
No CT + Fit	$0.933^{+0.321}_{-0.093}$	$-2.355^{+0.180}_{-0.200}$	60.88/33 (0.2%)	75.3	40.0
Gormley [10]					
	e_1	e_2 (GeV ⁻²)	χ^2/dof (Prob.)	η P.W. (eV)	η' P.W. (keV)
CT + No fit	0.222 ± 0.011	-1.203 ± 0.017	25.58/34 (85%)	56.3	48.9
CT + Fit	0.269 ± 0.080	$-1.275^{+0.135}_{-0.155}$	25.01/32 (80.6%)	54.6	47.7
No CT + No fit	0.222 ± 0.011	-1.203 ± 0.017	54.13/34 (1.6%)	76.9	53.4
No CT + Fit	0.529 ± 0.090	$-1.700^{+0.154}_{-0.195}$	36.38/32 (27.2%)	65.7	44.5

present exercise, we neglect model errors¹⁵; this mechanically makes the χ^2 look slightly more pessimistic than they really are.

We could have chosen to perform a simultaneous fit of the Crystal Barrel η' data set [23] together with both η data sets [10, 11] simultaneously. One could indeed imagine that the systematics could compensate. We have, nevertheless, preferred performing the fits separately for the Crystal Barrel η' spectrum together with each of these η spectra in isolation. Using both η spectra certainly leads to intermediate fit qualities.

Additionally, before letting e_1 and e_2 vary, we have performed the “0 parameter fit” in order to get the χ^2 and probabilities when using directly the parameter values as given in Table 1. In this way, we know the starting quality of the global description of these decay modes induced by the rest of the HLS phenomenology; we can also estimate what is gained by letting some parameters vary.

When using the data set of Layter et al. [11], while accounting for the η/η' contact terms at the expected level (assumption CT), one clearly sees from Table 4 that the ρ lineshape parameters e_1 and e_2 do not move farther than 2σ from the values found when fitting the pion form

¹⁵ These are certainly present as the uncertainties on a , g and x contribute to model errors, even when releasing any constraint on e_1 and e_2

factor [43] (the present σ are, however, much larger than found in fits to $F_\pi(s)$ [43]). The gain in χ^2 got by releasing these parameters is modest (2.7) and the central values for the partial widths get a little changed. This confirms that the parameter values in Table 1 giving $\chi^2/\text{dof} = 37.88/35$ (34% probability) are already close to optimum; leaving them free essentially improves the η spectrum lineshape slightly, but at the expense of slightly degrading the central values of the partial widths.

When dropping the contact term contributions (assumption NCT), the ρ lineshape parameters e_1 and e_2 change significantly with respect to their starting point, with much larger errors than originally. Even then, the fitted values for e_1 and e_2 move by more than 6 (new) σ from expectations; therefore, these fitted values can be considered inconsistent with their values fitted in the pion form factor. Additionally, even if the gain is large (χ^2/dof is improved from 140.65/35 to 60.88/33), it is not sufficient to push the probability (0.2%) to a reasonable value. Therefore, the peculiar uncertainties affecting this spectrum do not prevent one to reach a clear global conclusion.

When using the data set of Gormley et al. [10] together with the η' data of Crystal Barrel, the picture is unchanged, but looks much clearer. Fixing the parameters to their values in Table 1 gives already a remarkable fit quality (probability 85%), when contact terms are accounted for.

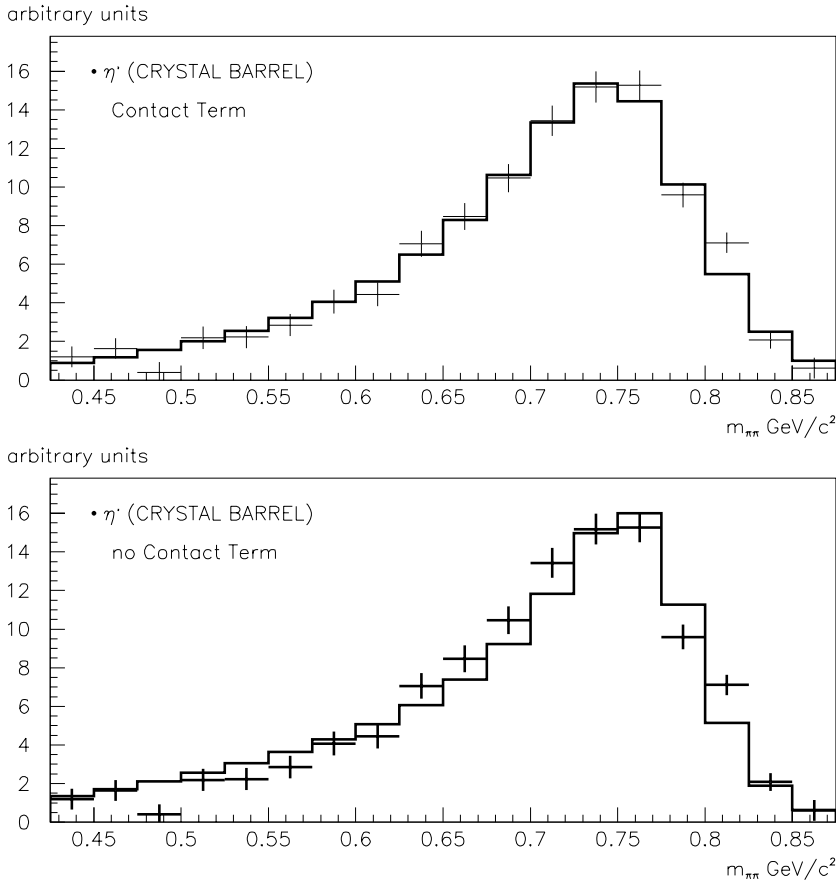


Fig. 6. Fit of the η' invariant mass spectrum; top by including the contact term, bottom by removing this term. Compare the peak locations

In this case, letting free e_1 and e_2 , the χ^2 improves a little (0.57 unit), but the fit probability degrades to 80%, because of the smaller number of degrees of freedom. The ρ parameters move by about 1 (new) σ from the expectations and thus stay consistent with the ρ lineshape determined when fitting the pion form factor [43] (the region of the minimum χ^2 seems flat).

When removing the contact term from our expressions (NCT assumption), the starting values of the fit parameters provide a comparatively poor description (1.6% probability) and the η partial width is far from expectations [9] (see also Table 4). Now, releasing e_1 and e_2 improves significantly the description, as we reach a 27% probability after the fit, with reasonable central values for both partial widths. The price to be paid for this configuration is that the parameters e_1 and e_2 change by more than 3 (new) σ from expectations. Therefore, the NCT assumption returns a ρ lineshape inconsistent with the fits to the pion form factor.

From the previous sections, we already knew that the CT assumption is certainly favored in a global account of both shape and partial width for both the η and η' mesons simultaneously. We also knew that the NCT assumption was disfavored under the same conditions.

What we have learnt in this section is that, in order to accommodate the description of all aspects of the η/η' information, the NCT assumption stops being consistent

with the ρ lineshape as found by fitting the pion form factor [43].

Therefore, we conclude that the experimental data do provide fair evidence in favor of the box anomaly phenomenon at the expected level; additionally, the sharing observed between resonant and contact term contributions ($-3 : 1$) is well predicted by the FKTUY assumption [30] leading to the Lagrangian in (5).

In Fig. 6, we show the description of the Crystal Barrel spectrum [23] using (24) (or (28)) with the contact term considered and removed. In order to get this we performed fits leaving free e_1 and e_2 .

When accounting for the η' contact term, the ρ peak location is found in the bin covering the mass region from 725 to 750 MeV. When dropping it, the (fit) mechanism described in Sect. 7.2 makes the ρ peak shift to the next bin which covers the mass interval from 750 to 775 MeV. This trend was already observed by [17, 23] and also by most Collaborations who have performed the extraction of the η' spectrum canonically; sometimes too much [15].

A real shift exists and is small (see Sect. 7.2). It is artificially increased by the fit procedure in order to get a better account of the low mass tail of the η' invariant-mass spectrum. However, this artificial large mass shift is indeed the signal of the box anomaly.

It is claimed in [24] that the L3 Collaboration does not observe a ρ peak shift. Several reasons can be invoked. First, as remarked above, [24] did not perform the η' spec-

Table 5. Simultaneous fit of the four HLS anomaly equations (see (11)) and (21) with only x free (approximate field transformation). The first data column gives the recommended values [9]

	PDG 2002	Fit result	Significance ($n\sigma$)
x		0.911 ± 0.015	
χ^2/dof		$2.66/3$	
Probability		44.6%	
$\Gamma(\eta \rightarrow \gamma\gamma)$ (keV)	0.46 ± 0.04	0.46 ± 0.01	0.00σ
$\Gamma(\eta' \rightarrow \gamma\gamma)$ (keV)	4.29 ± 0.15	4.34 ± 0.14	0.24σ
$\Gamma(\eta \rightarrow \pi^+\pi^-\gamma)$ (eV)	55 ± 5	56.64 ± 1.71	0.31σ
$\Gamma(\eta' \rightarrow \pi^+\pi^-\gamma)$ (keV)	60 ± 5	49.75 ± 3.88	1.62σ

trum extraction canonically and, therefore, any conclusion about the underlying ρ lineshape in the η' decay becomes a delicate matter.

Among other reasons the most likely is their fitting of the ρ mass and width. The ρ (Breit–Wigner) mass is thus found at values (766 ± 2 MeV) normally obtained only in processes where the dynamics is not really well under control (hadroproduction or photoproduction) [9].

If, for a moment, the L3 results were considered as a reference in order to detect a ρ peak shift, one might have instead to consider that a shift occurs in e^+e^- annihilations or τ decays, as these yield rather larger ρ (Breit–Wigner) masses ($\simeq 775$ MeV) [9]. Under these conditions, it is difficult to draw any conclusion from [24] about the existence (or absence) of a ρ peak location shift in the $\eta' \rightarrow \pi^+\pi^-\gamma$ decay.

11 Fits to the four anomaly equations

From now on, we make the assumption that the correct set of equations defining the anomalous amplitudes at the chiral limit are given by (11) and (21) and no longer by (3). These have been derived using the approximate field transformation (8). We also examine, for completeness, the case when the exact field transformation is used; the way to modify our anomaly equations to go from one case to the other is given in the Appendix.

In both cases, these equations actually depend on only one parameter (respectively x or λ); this can legitimately be looked upon as a severe constraint.

11.1 Fit results with approximate field transformation

These equations depend only on f_π , $z = [f_K/f_\pi]^2$ and on x . In the present framework, θ_P is no longer an independent parameter as can be algebraically derived from (10).

One can consider it legitimate to still fix f_π to its experimental value (92.42 MeV); this is also true for z (see Table 1). Therefore, our set of anomaly equations depends on only one parameter x we chose previously to fix from the fit results to radiative decays [32, 41]. Releasing the constraint (10) would only add a comfortable (and useless) parameter freedom to the fits presented below.

Therefore, one considers here (11) and (21) by themselves and attempts to fit them as a constrained system of four equations with only *one* unknown (x). The results are expected to provide consistency with those obtained for the same parameters and physical quantities derived elsewhere [32, 41] from a fit to the $VP\gamma$ decay modes.

The $\gamma\gamma$ partial widths are related with the amplitudes given in (11) by

$$\Gamma(X \rightarrow \gamma\gamma) = \frac{M_X^3}{64\pi} |G_X(0)|^2. \quad (30)$$

On the other hand, the partial widths $\Gamma(X \rightarrow \pi^+\pi^-\gamma)$ given by (27) where the coefficients A_X are given by (29), depend only on the ρ properties already derived in [43] by a fit to the pion form factor. The errors on A_X are taken into account in the fit as they are independent of x .

One has performed a fit of these four partial widths keeping first z fixed and allowing x to vary. The results are summarized in Table 5.

It is clear that the fit is fairly successful and represents the most constrained fit of the four partial widths ever proposed. One should remark that the best fit returns a value for x perfectly consistent with our previous fits solely to the $VP\gamma$ radiative decays, as can be concluded by comparing to its input value (see Table 1). The corresponding value for θ_P is not changed compared to our previous estimates from a fit to the $VP\gamma$ decay modes: $\theta_P = -10.48^\circ \pm 0.18^\circ$.

We do not give the estimates for the derived quantities (f_0 , f_8 , θ_0 , θ_8) as they practically coincide with the values given in [32] and are all in good correspondence with the expectations. Concerning partial widths, three out of four reach a significance much better than the 1σ level; the worst case is $\Gamma(\eta' \rightarrow \pi^+\pi^-\gamma)$ for which the distance to the recommended value [9] is “only” $\simeq 1.6\sigma$.

The fit quality yielded ($\chi^2/\text{dof} = 2.66/3$) is such that releasing also z can look like an academic exercise. It has nevertheless been performed as some correlation could numerically spoil the connection between z and $[f_K/f_\pi]^2$.

The fit returned $x = 0.908 \pm 0.021$ and $z = 1.488 \pm 0.054$ with $\chi^2/\text{dof} = 2.62/2$, practically unchanged, corresponding to a 27% probability (the worse significance is due to having less degrees of freedom). The correlation coefficient is +0.67, and the minimization does not spoil the numerical values found elsewhere [32, 41] for the same parameters.

Table 6. Simultaneous fit of the four HLS anomaly equations modified by using the exact field transformation. The second data column reports on letting free λ and θ_P , while in the third data column only λ is allowed to vary

	PDG 2002	Fit result θ_0 free	Fit result $\theta_0 = 0$
λ		0.23 ± 0.06	0.21 ± 0.04
θ_P		$-10.85^\circ \pm 1.27^\circ$	$-11.48^\circ \pm 0.02^\circ$
χ^2/dof		2.93/2	3.20/3
Probability		23.1%	36.5%
θ_0		$-1.01^\circ \pm 1.27^\circ$	0
θ_8		$-19.37^\circ \pm 1.29^\circ$	$-18.16^\circ \pm 0.24^\circ$
f_0		1.37 ± 0.03	1.36 ± 0.03
f_8		1.34 ± 0.01	1.34 ± 0.02
$\Gamma(\eta \rightarrow \gamma\gamma)$ (keV)	0.46 ± 0.04	0.45 ± 0.03	0.44 ± 0.01
$\Gamma(\eta' \rightarrow \gamma\gamma)$ (keV)	4.29 ± 0.15	4.37 ± 0.23	4.20 ± 0.17
$\Gamma(\eta \rightarrow \pi^+\pi^-\gamma)$ (eV)	55 ± 5	55.38 ± 2.78	55.98 ± 1.76
$\Gamma(\eta' \rightarrow \pi^+\pi^-\gamma)$ (keV)	60 ± 5	49.40 ± 4.85	46.93 ± 4.00

Therefore, this leads us to conclude that the $VP\gamma$ decay modes on the one hand, and the four standard anomalous η/η' decay modes on the other hand, yield information fairly consistent with each other. This also means that the anomaly equations we derived are consistent and that the approximate field transformation (leading order in breaking parameters) on which they rely match well the present level of accuracy of the data. This statement will be confirmed directly shortly.

11.2 θ_P versus x

Equation (10) corresponds to setting the EChPT decay constant [2, 3] F_η^0 to zero. This is rigorously expressed in the broken HLS model by

$$\tan \theta_P = \frac{\langle 0 | J_\mu^0 | \eta^8(q) \rangle}{\langle 0 | J_\mu^0 | \eta^0(q) \rangle} = \frac{b_0}{f_0} \quad (31)$$

in terms of current matrix elements and of their expressions [32]. On the other hand, detailed computation yields

$$\frac{f_0}{f_\pi} = \frac{2+z}{3x}, \quad \frac{b_0}{f_\pi} = \frac{\sqrt{2}}{3} (1-z) x. \quad (32)$$

As clear from its expression f_0 keeps the first non-leading contribution in the breaking parameters ($x = 1 + [x - 1]$); for b_0 one has naturally chosen to replace x by 1 and this leads to (10). However, one may be tempted to keep it and this leads one to replace x by x^2 in the expression (10) for $\tan \theta_P$; this is nothing but changing the existing term of order $\mathcal{O}([z - 1][x - 1]) \simeq 0.05$.

We have redone the fit just described with this change and this yielded a slightly better fit quality than the previous one ($\chi^2/\text{dof} = 2.61/3$). This fit returns also $x = 0.902 \pm 0.017$ ($\simeq 0.5 \sigma$ from its partner in Table 5,

or also a one percent change) and no change at all for the partial widths compared to what is displayed in Table 5.

Therefore the sensitivity in describing the data is not sharply dependent on non-leading contributions in $\tan \theta_P$ and using (10) with x or x^2 gives undistinguishable results, while the latter might be preferred.

11.3 Fit results with exact field transformation

In order to check the sensitivity of the model to some other details of the broken HLS model, we have also attempted fits using the exact field transformation [32] instead of its leading order approximation (see (8)); some details and formulae are given in the Appendix.

The main motivation was to figure out the sensitivity of the data to the approximation performed on the field transformation.

In this last series of fits, we have kept z fixed; therefore the fitting parameters are λ (the basic nonet symmetry breaking parameter; see (7)) and θ_P , the latter being possibly fixed by the constraint $\theta_0 = 0$. The fit results and physical quantities of relevance (ChPT decay constants, mixing angles and partial widths) are given in Table 6.

The first conclusion one can draw from this last table is that the fit value for θ_0 departs by less than 1σ from zero and the consequences of this on the derived physical quantities is simply negligible. Stated otherwise, the present data are insensitive to releasing the constraint $\theta_0 = 0$. This constraint allows one to extract a value for $\theta_8 = -18.2^\circ$ with a very small statistical error ($\simeq 0.25^\circ$); the values found for f_0 and f_8 are in the usual ballpark and nothing noticeable appears compared to the case when the approximate field transform was used [32].

The partial widths are still quite consistent with those in Table 5, showing that the refinements introduced by the exact transformation have no impact on the extracted width information for $\eta/\eta' \rightarrow \gamma\gamma$ and $\eta/\eta' \rightarrow \pi^+\pi^-\gamma$.

One might maybe note that, in all our attempts, we never get a solution with the partial width for $\eta' \rightarrow \pi^+\pi^-\gamma$ larger than its recommended value [9]; so, the observed 1.6σ departure looks like some small systematic effect. This could be due to having neglected some unidentified tiny (higher order) contribution; this might also indicate that the recommended value is slightly overestimated.

On the other hand, we have also reconsidered the problem of which value for $\eta \rightarrow \gamma\gamma$ should be preferred among the recommended value [9] – recently confirmed by a direct measurement of this branching fraction [66] –, the $\gamma\gamma$ measurements and the (single) Primakoff effect measurement. This was done already in [32], but with only the $\eta/\eta' \rightarrow \gamma\gamma$ modes. In the present framework extended to the $\eta/\eta' \rightarrow \pi^+\pi^-\gamma$ decay modes, the conclusion is confirmed: The recommended value is still clearly preferred; the fit quality indicates that it could be slightly smaller (in the direction of the Primakoff measurement), but larger values (in the direction of the $\gamma\gamma$ measurements) are clearly disfavored.

12 Summary and conclusion

The conclusions we get are of various kinds. Therefore, we prefer segmenting the following into subsections.

Experimental relevance of the box anomaly

Concerning the analysis of a possible occurrence of the box anomaly phenomenon in η/η' decays, the main results reported in the present paper can be summarized as follows.

(1) There is strong evidence in favor of a contact term contribution in the η/η' decays to $\pi^+\pi^-\gamma$. All aspects (invariant-mass spectra and partial widths) of the $\eta/\eta' \rightarrow \pi^+\pi^-\gamma$ decays can be *predicted* with a fair accuracy using a few pieces of information coming from fits to $VP\gamma$ and Ve^+e^- decay modes in isolation and from information coming from a fit to the pion form factor.

(2) The needed contact term is numerically at the precise value predicted for the box anomaly contribution by the anomalous HLS Lagrangian. This plays a crucial role in yielding, without any fit, the correct dipion invariant-mass spectra and the correct partial widths for both the η and η' mesons.

(3) If one lets free the parameters defining the ρ meson lineshape in the η/η' spectra, they stay very close to the values expected from (independent) fits to the pion form factor if the predicted contact term is switched on.

In contrast, if one removes this from the amplitudes, the description is poor and can only be improved by letting the ρ lineshape becoming inconsistent with what is expected from fits to the pion form factor.

(4) The fit value obtained for the single free parameter (x , accounting essentially for nonet symmetry breaking) indicates beyond doubt that a global description of all $VP\gamma$ modes and of the four η/η' decay modes examined here is derived with no additional free parameter.

This leads us to conclude to strong evidence in favor of the occurrence of the box anomaly phenomenon in $\eta/\eta' \rightarrow \pi^+\pi^-\gamma$ decays at precisely the level expected from the HLS model and the WZW Lagrangian.

Anomaly equations and mixing angles

On the other hand, we have been led to reexamine the validity of the one-angle traditional equations giving the amplitudes for $\eta/\eta' \rightarrow \gamma\gamma$ and $\eta/\eta' \rightarrow \pi^+\pi^-\gamma$ at the chiral point, when breaking flavor SU(3) and nonet symmetries, respectively, the triangle and box anomaly equations.

We have found that the broken HLS model leads to one-angle (θ_P) expressions for the anomaly equations which match low energy QCD expectations as expressed by (E)ChPT, but are in deep contradiction with the equations traditionally used.

Instead of depending on three unconstrained parameters, this set of (four) equations we get depends on only one parameter, closely associated with nonet symmetry breaking (called x or λ in the body of the text); they also depend on $z = [f_K/f_\pi]^2$ which can hardly be considered as a free parameter. They are proved to be easily fulfilled by the relevant η/η' partial widths with fair accuracy.

Relying on the condition $\theta_0 = 0$, well accepted by the existing data, the broken HLS model leads to an expression of θ_P in terms of z and x (or λ) which can be approximated by a simple formula. Additionally, under the same assumption, an equation leading to $\theta_8 \simeq 2\theta_P$ can be derived.

These equations have been derived from within the framework of the hidden local symmetry model appropriately broken. The phenomenological success of this mechanism implies that the BKY SU(3) symmetry breaking scheme, supplemented with nonet symmetry breaking can be considered as the relevant breaking mechanism.

This extended BKY breaking scheme forces one to a field transformation which admits a reliable approximation valid at leading order in the breaking parameters ($[z - 1]$, $[x - 1]$). The refinements permitted by the exact transformation are found to be beyond the present accuracy of the experimental data.

Perspectives

At the level of accuracy permitted by the existing data, the HLS model (including its anomalous sector), together with the extended BKY symmetry breaking scheme, covers successfully all aspects of the experimental data examined so far, certainly up to the ϕ mass.

It would be interesting to have improved data in order to check up to which accuracy the HLS framework is predictive. For this purpose, more and better data on the η/η' sector would be welcome.

These could come from tau-charm factories (CLEO-C and upgraded BESS) which, running at the $J/\psi(1S)$, produce very large samples of η/η' mesons under especially clean physics conditions. For instance, in the run at the

$J/\psi(1S)$ foreseen by CLEO-C in 2005 10^9 events will be collected. This will provide 860 000 η produced opposite in azimuth to a single monoenergetic photon and 2 000 000 opposite to ω/ϕ . The corresponding η' decay modes will provide samples of about 4 300 000 η' produced opposite to a single photon and 500 000 opposite to ω/ϕ . This should allow an exhaustive study to be made of the η/η' system and a much better understanding of low energy QCD.

Acknowledgements. We gratefully acknowledge V.L. Chernyak (Budker Institute, Novosibirsk) for a critical reading of the manuscript and for valuable remarks and comments. We also acknowledge G. Shore (Swansea University, UK) for useful correspondence and reading the manuscript. Fermilab is operated by URA under DOE contract No. DE-AC02-76CH03000.

Appendix

A1 The exact field transformation

As stated in Sect. 4, the field transformation given by (8) is an approximation of the full transformation which has been derived in [32].

In order to bring the kinetic energy part of the $U(3)/SU(3)$ broken HLS Lagrangian into canonical form (see (7)), it is appropriate to perform the renormalization in two steps. One first diagonalizes the standard \mathcal{L}_{HLS} piece using the field transformation (6). This makes the Lagrangian canonical for the π/K sector, and one yields intermediate fields for the isoscalar sector (double prime fields). In terms of bare fields, we have

$$\begin{bmatrix} \eta''_8 \\ \eta''_0 \end{bmatrix} = zr \begin{bmatrix} \cos \beta & -\sin \beta \\ -\sin \beta & \cos \beta - \frac{1}{\sqrt{2}} \sin \beta \end{bmatrix} \begin{bmatrix} \eta_8 \\ \eta_0 \end{bmatrix}, \quad (33)$$

where one has defined

$$r = \frac{\sqrt{(2z+1)^2 + 2(z-1)^2}}{3z} \simeq 0.90, \quad \tan \beta = \sqrt{2} \frac{z-1}{2z+1} \simeq 0.20. \quad (34)$$

This transformation brings the kinetic term in the following form [32]:

$$2T = [\partial\eta''_8]^2 + [\partial\eta''_0]^2 + \lambda r [\sin \beta \partial\eta''_8 + \cos \beta \partial\eta''_0]^2. \quad (35)$$

The transformation to fully renormalized fields (primed fields) is performed with

$$\begin{bmatrix} \eta'_8 \\ \eta'_0 \end{bmatrix} = \begin{bmatrix} 1 + v \sin^2 \beta & v \sin \beta \cos \beta \\ v \sin \beta \cos \beta & 1 + v \cos^2 \beta \end{bmatrix} \begin{bmatrix} \eta''_8 \\ \eta''_0 \end{bmatrix}, \quad (36)$$

where v carries the real information about the nonet symmetry breaking (see (7)):

$$v = \sqrt{1 + \lambda r^2} - 1 \simeq 0.10. \quad (37)$$

That the transformation combining (33) and (36) results, at leading order in the breaking parameters $[z-1]$ and $[x-1]$, in a transformation as simple as (8) is a little bit unexpected. As noted in the main text, there are several combinations involving λ which are equivalent to x at leading order; they are all of the form exhibited by (9) which is typically a good representation of x in terms of λ .

This remainder makes clear why x is influenced by the $SU(3)$ symmetry breaking. A typical expression for x is

$$x = \frac{1}{\sqrt{1+v}}. \quad (38)$$

A2 The anomalous amplitudes at the chiral limit

The expressions for the anomalous amplitudes at the chiral limit, when using the exact transformation, are easy to get. They amount to the following changes for the triangle anomaly expressions in (11):

$$\begin{aligned} \frac{5z-2}{3z} &\Rightarrow \frac{1}{1+v} \left[\frac{5z-2}{3z} + \frac{v \cos \beta}{rz} \right] && \text{(octet)}, \\ \sqrt{2} \frac{5z+1}{3z} x &\Rightarrow \frac{1}{1+v} \left[\sqrt{2} \frac{5z+1}{3z} - \frac{v \sin \beta}{rz} \right] && \text{(singlet)}. \end{aligned} \quad (39)$$

The octet and singlet combinations for the box anomalies can easily be identified by the occurrence of the x factor in (19) and (21). The changes to be performed there are

$$\begin{aligned} 1 &\Rightarrow \frac{1}{1+v} \left[1 + \frac{v \cos \beta}{rz} \right] && \text{(octet)}, \\ x &\Rightarrow \frac{1}{1+v} \left[1 - \frac{v \sin \beta}{rz\sqrt{2}} \right] && \text{(singlet)}. \end{aligned} \quad (40)$$

It is worth remarking that the exact field transformation changes the $(\rho\eta)$ and $(\rho\eta')$ coupling constants in such a way that the c_X – modified as just stated – still factor out from their expression. Therefore, (18) and (24) keep their structure and the decay invariant-mass spectra for the η/η' are the same as for the approximate field transformation.

A3 Decay constants and mixing angles

One can easily express the EChPT coupling constants (f_0 and f_8) and mixing angles (θ_0 and θ_8) in terms of the parameters mixing λ and β defined in the previous subsections.

The following matrix elements of axial currents can be defined in the broken HLS Lagrangian [32]:

$$\begin{aligned} \langle 0 | J_\mu^8 | \pi^8(q) \rangle &= if_8 q_\mu, & \langle 0 | J_\mu^0 | \eta^0(q) \rangle &= if_0 q_\mu, \\ \langle 0 | J_\mu^8 | \eta_0(q) \rangle &= ib_8 q_\mu, & \langle 0 | J_\mu^0 | \pi^8(q) \rangle &= ib_0 q_\mu. \end{aligned} \quad (41)$$

One can easily write down the currents and their matrix elements (see [32], Sect. 6) in the case when the field transformation is not approximated by (8). Using the notation defined in [32], one finds first

$$\begin{aligned}\frac{f_8}{f_\pi} &= \frac{rz}{1+v} [1 + v \cos 2\beta] \cos \beta, \\ \frac{b_8}{f_\pi} &= -\frac{rz}{1+v} [1 - v \cos 2\beta] \sin \beta.\end{aligned}\quad (42)$$

Defining the following parameter combinations:

$$\begin{aligned}h_1 &= \cos \beta - \frac{\sin \beta}{\sqrt{2}} \simeq 0.90, \\ h_2 &= \lambda \cos \beta - \frac{1+\lambda}{\sqrt{2}} \sin \beta \simeq 0.03,\end{aligned}\quad (43)$$

one also finds

$$\begin{aligned}\frac{f_0}{f_\pi} &= \frac{rz}{1+v} [h_1(1+\lambda) + v(2 \cos \beta + h_2) \sin^2 \beta], \\ \frac{b_0}{f_\pi} &= -\sin \beta \frac{rz}{1+v} [(1+v \cos 2\beta) - h_1 v \cos \beta].\end{aligned}\quad (44)$$

A4 The condition $\theta_0 = 0$

Phenomenology [32] as well as explicit EChPT computations [58] indicate that the mixing angle θ_0 is very close to zero. Table 6 clearly illustrates that the present data are statistically insensitive to letting θ_0 depart from zero. Under such conditions, several interesting relations show up.

The definition of the angles θ_0 and θ_8 can be expressed in terms of the parameters in (41) [32]. Using (44), one can derive

$$\tan \theta_8 = \tan(\theta_P + \varphi_8), \quad \tan \theta_0 = -\tan(\theta_P - \varphi_0) \quad (45)$$

where $\tan \varphi_8 = b_8/f_8$ and $\tan \varphi_0 = b_0/f_0$ can be explicitly computed. The condition $\theta_0 = 0$ strictly implies that $\theta_P = \varphi_0$, which gives

$$\tan \theta_P = -\frac{1}{1+\lambda} \left[\frac{\tan \beta}{1 - \frac{1}{\sqrt{2}} \tan \beta} \right] \left[1 + \frac{v \tan \beta}{\sqrt{2}} + \dots \right]. \quad (46)$$

From (38), the first term can be interpreted as x^2 and the product of the first two factors is just (10) for $\tan \theta_P$ modified with x^2 . With the values for v and $\tan \beta$ we have mentioned, the leading correction amounts to only $1.5 \cdot 10^{-2}$. If one keeps a $1/\sqrt{1+\lambda}$ (corresponding to having x in (10)) in front of this expression, the correction term gets a additional contribution $-\lambda/2 \simeq 5 \cdot 10^{-2}$ which becomes dominant. Therefore

$$\tan \theta_P = \sqrt{2} \frac{(1-z)}{2+z} x^2 \quad (47)$$

could indeed be preferred to (10).

The second information which follows from $\theta_0 = 0$ is an approximate relation between θ_8 and the wave-function mixing angle θ_P :

$$\tan \theta_8 = 2 \tan \theta_P \left[1 - \frac{\tan \beta}{2\sqrt{2}} + \dots \right], \quad (48)$$

where the leading correction is $\simeq 7 \cdot 10^{-2}$.

References

1. J. Gasser, H. Leutwyler, *Annals Phys.* **158**, 142 (1984); *Nucl. Phys. B* **250**, 465 (1985)
2. H. Leutwyler, *Nucl. Phys. Proc. Suppl.* **64**, 223 (1998) [hep-ph/9709408]
3. R. Kaiser, H. Leutwyler, Pseudoscalar decay constants at large $N(c)$, hep-ph/9806336; *Eur. Phys. J. C* **17**, 623 (2000) [hep-ph/0007101]
4. J. Wess, B. Zumino, *Phys. Lett. B* **37**, 95 (1971)
5. E. Witten, *Nucl. Phys. B* **223**, 422 (1983)
6. V.V. Solovov, M.V. Terentev, *Sov. J. Nucl. Phys.* **16**, 82 (1973) [*Yad. Fiz.* **16**, 153 (1972)]
7. Y.M. Antipov et al., *Phys. Rev. D* **36**, 21 (1987)
8. B.R. Holstein, *Phys. Scripta T* **99**, 55 (2002) [hep-ph/0112150]
9. K. Hagiwara et al. [Particle Data Group Collaboration], *Phys. Rev. D* **66**, 010001 (2002)
10. M. Gormley, E. Hyman, W.Y. Lee, T. Nash, J. Peoples, C. Schultz, S. Stein, *Phys. Rev. D* **2**, 501 (1970)
11. J.G. Layter, J.A. Appel, A. Kotlewski, W.Y. Lee, S. Stein, J.J. Thaler, *Phys. Rev. D* **7**, 2565 (1973)
12. A. Grigorian et al., *Nucl. Phys. B* **91**, 232 (1975)
13. M. Althoff et al. [TASSO Collaboration], *Phys. Lett. B* **147**, 487 (1984)
14. H. Albrecht et al. [ARGUS Collaboration], *Phys. Lett. B* **199**, 457 (1987)
15. H. Aihara et al. [TPC/Two Gamma Collaboration], *Phys. Rev. D* **35**, 2650 (1987)
16. G. Gidal et al. [MarkII Collaboration] in *Multiparticle Dynamics 1985, Proceedings of the XVIIth International Symposium at Kyriat Anavim (Israel)*, edited by J. Grunhaus (Editions Frontières, Gif-sur-Yvette, France 1987)
17. S.I. Bityukov et al., *Z. Phys. C* **50**, 451 (1991)
18. T.A. Armstrong et al. [WA76 Collaboration], *Z. Phys. C* **54**, 371 (1992)
19. M. Feindt, [PLUTO Collaboration], *Research On Two Photon Production Of Eta-Prime Mesons With The Pluto Detector*, DESY-PLUTO-84-03
20. F. Butler [MarkII Collaboration], *Resonant Production In Two Photon Collisions*, LBL preprint FCE 26465, Ph.D. Thesis, Berkeley 1988
21. K.W. McLean [ARGUS Collaboration], *Desy Preprint F 15-90-03*, Ph.D. Thesis, Hamburg 1990
22. J.H. Peters [CELLO Collaboration], *Production Of Eta, Eta-Prime And F1(1285) Mesons In Tagged And Untagged Two Photon Reactions*, DESY-FCE-90-01
23. A. Abele et al. [Crystal Barrel Collaboration], *Phys. Lett. B* **402**, 195 (1997)
24. M. Acciarri et al. [L3 Collaboration], *Phys. Lett. B* **418**, 399 (1998)
25. G. Ecker, J. Gasser, H. Leutwyler, A. Pich, E. de Rafael, *Phys. Lett. B* **223**, 425 (1989)

26. O. Kaymakcalan, S. Rajeev, J. Schechter, Phys. Rev. D **30**, 594 (1984); O. Kaymakcalan, J. Schechter, Phys. Rev. D **31**, 1109 (1985)
27. P. Jain, R. Johnson, U.G. Meissner, N.W. Park, J. Schechter, Phys. Rev. D **37**, 3252 (1988)
28. U.G. Meissner, Phys. Rept. **161**, 213 (1988)
29. M. Bando, T. Kugo, K. Yamawaki, Phys. Rept. **164**, 217 (1988)
30. T. Fujiwara, T. Kugo, H. Terao, S. Uehara, K. Yamawaki, Prog. Theor. Phys. **73**, 926 (1985)
31. G. Ecker, J. Gasser, H. Leutwyler, A. Pich, E. de Rafael, Phys. Lett. B **223**, 425 (1989)
32. M. Benayoun, L. DelBuono, H.B. O'Connell, Eur. Phys. J. C **17**, 593 (2000) [hep-ph/9905350]
33. M. Benayoun, M. Feindt, M. Girone, A. Kirk, P. Leruste, J.L. Narjoux, K. Safarik, Z. Phys. C **58**, 31 (1993)
34. M. Benayoun, P. Leruste, L. Montanet, J.L. Narjoux, Z. Phys. C **65**, 399 (1995)
35. M.S. Chanowitz, Phys. Rev. Lett. **35**, 977 (1975); **44**, 59 (1980)
36. F.J. Gilman, R. Kauffman, Phys. Rev. D **36**, 2761 (1987) [Erratum D **37**, 3348 (1988)]
37. J.F. Donoghue, B.R. Holstein, E. Golowich, Dynamics of the standard model (Cambridge University Press, New York 1992)
38. E.P. Venugopal, B.R. Holstein, Phys. Rev. D **57**, 4397 (1998) [hep-ph/9710382]
39. M. Bando, T. Kugo, K. Yamawaki, Nucl. Phys. B **259**, 493 (1985)
40. M. Benayoun, H.B. O'Connell, Phys. Rev. D **58**, 074006 (1998) [hep-ph/9804391]
41. M. Benayoun, L. DelBuono, S. Eidelman, V.N. Ivanchenko, H.B. O'Connell, Phys. Rev. D **59**, 114027 (1999) [hep-ph/9902326]
42. M. Benayoun, L. DelBuono, Ph. Leruste, H.B. O'Connell, Eur. Phys. J. C **17**, 303 (2000) [nucl-th/0004005]
43. M. Benayoun, L. DelBuono, P. David, Ph. Leruste, H.B. O'Connell, The Pion Form Factor Within the Hidden Local Symmetry Model [nucl-th/0301037], to be published in Eur. Phys. J. C
44. M. Benayoun, S. Eidelman, K. Maltman, H.B. O'Connell, B. Shwartz, A.G. Williams, Eur. Phys. J. C **2**, 269 (1998) [hep-ph/9707509]
45. S. Rudaz, Phys. Rev. D **41**, 2619 (1990)
46. A. Abbas, Phys. Lett. B **238**, 344 (1990); On the number of colours in quantum chromodynamics, [hep-ph/0009242]
47. O. Bar, U.J. Wiese, Nucl. Phys. B **609**, 225 (2001) [hep-ph/0105258]
48. O. Hajuj, Z. Phys. C **60**, 357 (1993)
49. C. Picciotto, Phys. Rev. D **45**, 1569 (1992)
50. T. Feldmann, Int. J. Mod. Phys. A **15**, 159 (2000) [hep-ph/9907491]
51. T. Feldmann, P. Kroll, Phys. Scripta T **99**, 13 (2002) [hep-ph/0201044]
52. M.N. Achasov et al. [SND Collaboration], Phys. Rev. D **65**, 032002 (2002) [hep-ex/0106048]
53. A. Aloisio et al. [KLOE Collaboration], Phys. Lett. B **561**, 55 (2003) [hep-ex/0303016]
54. R.R. Akhmetshin et al. [CMD-2 Collaboration], Phys. Lett. B **415**, 445 (1997)
55. M. Benayoun, H.B. O'Connell, Eur. Phys. J. C **22**, 503 (2001) [nucl-th/0107047]
56. G. 't Hooft, Phys. Rept. **142**, 357 (1986)
57. P.J. O'Donnell, Rev. Mod. Phys. **53**, 673 (1981)
58. J.L. Goity, A.M. Bernstein, B.R. Holstein, Phys. Rev. D **66**, 076014 (2002) [hep-ph/0206007]
59. C. McNeile, C. Michael [UKQCD Collaboration], Phys. Lett. B **491**, 123 (2000) [hep-lat/0006020]
60. R.R. Akhmetshin et al. [CMD-2 Collaboration], Phys. Lett. B **527**, 161 (2002) [hep-ex/0112031]
61. J.J. Sanz-Cillero, A. Pich, Eur. Phys. J. C **27**, 587 (2003) [hep-ph/0208199]
62. F. Butler et al. [MarkII Collaboration], Phys. Rev. D **42**, 1368 (1990)
63. H.B. O'Connell, B.C. Pearce, A.W. Thomas, A.G. Williams, Phys. Lett. B **336**, 1 (1994) [hep-ph/9405273]
64. B. Ananthanarayan, B. Moussallam, JHEP **0205**, 052 (2002) [hep-ph/0205232]
65. B. Mecking et al., Study of the Axial Anomaly using the $\gamma\pi^+ \rightarrow \pi^+\pi^0$ Reaction near threshold, CEBAF, Exp. 94-015, Newport News, 1994
66. R. Abegg et al., Phys. Rev. D **53**, 11 (1996)